1960

Conformal mapping of cylindrical cascades by means of an electrical analog

Rothrock, George B.

Monterey, California: U.S. Naval Postgraduate School

CONFORMAL MAPPING OF CYLINDRICAL CASCADES BY MEANS OF AN ELECTRICAL ANALOG

GEORGE B. ROTHROCK, JR.
and
ERNEST E. TISSOT, JR.

CONFORMAL MAPPING OF CYLINDRICAL CASCADES BY MEANS OF AN ELECTRICAL ANALOG

* * * * * * * * * * * * * * *

George B. Rothrock, Jr.

and

Ernest E. Tissot, Jr.

CONFORMAL MAPPING OF CYLINDRICAL CASCADES BY MEANS OF AN ELECTRICAL ANALOG

by

George B. Rothrock, Jr.
Lieutenant Commander, United States Navy

and

Ernest E. Tissot, Jr.
Lieutenant Commander, United States Navy

Submitted in partial fulfillment of
the requirements for the degree of

MASTER OF SCIENCE
IN
AERONAUTICAL ENGINEERING

United States Naval Postgraduate School
Monterey, California

1 9 6 0

CONFORMAL MAPPING OF CYLINDRICAL CASCADES BY MEANS OF AN ELECTRICAL ANALOG

by

George B. Rothrock, Jr.

and

Ernest E. Tissot, Jr.

This work is accepted as fulfilling

the thesis requirements for the degree of

MASTER OF SCIENCE

IN

AERONAUTICAL ENGINEERING

from the

United States Naval Postgraduate School

ABSTRACT

An attempt to predict the performance of a cylindrical cascade under actual operating conditions in the diffuser of a turbomachine was made by investigating the potential flow of an ideal fluid through the same cascade. The performance criteria used were the cascade turning angles and the pressure distribution about the cascade blade profiles at various cascade flow inlet angles. The potential flow of an ideal fluid was investigated by means of conformal transformations in conjunction with an electrical analog. Results indicate that the actual operating conditions of the cascade in the turbomachine vary to such a great extent from the conditions required of a potential flow that no reasonably accurate predictions of cascade performance can be made. A proposed line of investigation is suggested in order to develop the techniques necessary for a more accurate prediction of cylindrical cascade performance.

This investigation was conducted during the Spring of 1960 under the guidance of Professor M. H. Vavra of the U. S. Naval Postgraduate School, Monterey, California. The authors wish to express their appreciation to Professor Vavra for his assistance and encouragement during this investigation.

TABLE OF CONTENTS

TABLE OF CONTENTS

TABLE OF CONTENTS

TABLE OF CONTENTS

1. INTRODUCTION

Essential to the design of turbomachines is the design of the fixed and rotating cascades which compose the elemental parts of these machines. Several cascade design techniques are based on the assumption that the actual three-dimensional performance of the cascade may be approximated without serious error by the two-dimensional flow of an ideal fluid through the same cascade. An ideal fluid is defined herein as a fluid that is homogeneous, continuous, incompressible, and inviscid.

The object of this investigation is to compare two of the basic performance parameters of a cylindrical cascade resulting from the two-dimensional flow of an ideal fluid with those obtained from the flow of air through the same cascade in an actual turbomachine. Cylindrical cascade, as used here, refers to a cascade whose axis in the two-dimensional representation forms a circle and the surface generated by this axis in forming a three-dimensional cascade is a right circular cylinder. The axis of a cascade is a line or curve which passes through the identical point on each of the equally spaced blades which form the cascade.

At the present time no practical mathematical methods have been developed to treat ideal fluid flows through cascades of arbitrary configurations. The method used in this investigation involves the use of an electric analog in conjunction with conformal mapping. This method

was developed by Fahland and Hawkins in Ref. 1 and is described in considerable detail in Ref. 2. While the use of an electrical analog introduces an element of experimental error into the theoretical solution it should be remembered that this solution is used as an approximation to the actual flow and need not be an exact solution.

The actual cascade which was studied and its associated turbomachine are located at the U. S. Naval Postgraduate School, Monterey, California. Since the cascade was a cylindrical cascade, an additional conformal transformation was required to transform it into a rectilinear cascade which would be suitable for use with the electrical analog method. This transformation was devised by Professor M. H. Vavra. The inverse of this transformation was used to convert the results obtained for the rectilinear cascade to the values appropriate to the cylindrical cascade.

The basic method chosen to compare the performance of the cascade under the ideal and actual flow conditions was the pressure distribution around a blade profile. This method of comparison was chosen because of its fundamental nature and because several cascade design criteria of allowable blade loading are based on pressure maps constructed in various ways from this basic data. Pressure distribution data also provides means of determining Mach number limitations and evaluating the profile losses of axial flow compressor cascades. The second parameter which was the basis for comparison was that of cascade turning angle.

This work was conducted at the U. S. Naval Postgraduate School, Monterey, California, during the Spring of 1960. The authors wish to express their sincere appreciation to Professor M. H. Vavra of the U. S. Naval Postgraduate School for his stimulating and rewarding guidance. This thesis project was conceived by Professor Vavra and is an extended application of previous investigative work performed under his supervision.

2. TABLE OF SYMBOLS

b	distance from origin of sources and sinks, φ plane
c	blade chord length
i	indicates imaginary part in complex number notation
L	leading edge point of profile chord reference lines, w and z planes
M	flow stagnation points, z and φ planes
N	number of blades in cylindrical cascade
p	static pressure
P	arbitrary point on blade profile
Q	arbitrary point on blade profile
r	radius vector length, w plane
s	blade spacing in rectilinear cascade
S	pressure coefficient
T	trailing edge point of blade profile, w, z and φ planes
V	velocity
w	complex variable
x	abscissa, z plane
X	abscissa, w plane
y	ordinate, z plane
Y	ordinate, w plane
z	complex variable
α	angle of fluid flow

α_1 cascade inlet flow angle

α_2' cascade exit angle of reference flow at the trailing edge

α_3 cascade exit angle of flow downstream from trailing edge

α_3' cascade exit angle of uniform flow downstream from trailing edge

α_∞ angle of vectorial mean of inlet and exit velocity vectors, rectilinear cascade

α_i angle of incidence

$\Delta\alpha$ cascade turning angle, $\alpha_1 - \alpha_2'$

β polar angle of trailing edge point, φ plane

γ polar angle, w plane

δ stagger angle, cylindrical cascade

ξ stagger angle, rectilinear cascade

φ complex variable

η ordinate, φ plane

η_c conventional profile coordinate, w plane

η_r conventional profile coordinate, z plane

θ polar angle, φ plane

λ arc corresponding to one blade space, cylindrical cascade

ξ abscissa, φ plane

ξ_c conventional profile coordinate, w plane

ξ_r conventional profile coordinate, z plane

ρ fluid density

σ solidity, rectilinear cascade $(\frac{c}{s})$

ϕ	electrical or fluid potential
$\bar{\Phi}$	non-dimensional volumetric flow rate in Compressor Test Rig

Subscripts:

1	upstream of cascade
2	at trailing edge of cascade
3	downstream of cascade
a	direction perpendicular to rectilinear cascade axis
c	pertaining to cylindrical cascade
i	incidence or inner
L	pertaining to leading edge point of profile
o	outer
r	pertaining to rectilinear cascade
R	pertaining to radial direction, w plane
t	pertaining to tangential direction, w plane
T	pertaining to trailing edge point of profile
w	pertaining to w plane
z	pertaining to z plane

Superscripts:

'	pertaining to the hypothetical uniform flow

3. THE IDEAL FLOW

3.1 INTRODUCTION

If, in addition to the requirements of the definition of an ideal fluid and two-dimensional flow, the condition of irrotationality is imposed on the ideal fluid approaching a cascade, the techniques which apply to potential flow may be used to obtain a solution to the flow field. Several exact solutions for potential flows through cascades composed of thin blades with small camber have been devised using conformal mapping techniques; however, no practical solutions for arbitrary cascade configurations are available at the present time. The exact solutions, while not directly applicable here, do show that rectilinear cascades may be transformed into a single closed curve in a complex plane with a suitable source-sink distribution Such a plane is shown in Fig. 1b with sources and sinks located on the real axis. The closed curve resulting from this configuration is a circle. The complex potential function may be expressed for this plane and equipotential lines may be constructed over the entire plane. The potential distribution about the circumference of the circle is of particular interest here.

The use of an electric analog as developed in Ref. 1 permits the determination of equipotential lines for a potential flow through the rectilinear cascade under investigation. The analog consists of a flat sheet of paper of uniform electrical conductivity from which the desired cascade has been cut out. The conditions of potential flow are satisfied by the flow of direct current electricity between two bus bars located on

each side of the cascade axis. The equipotential lines are constructed by measurement of the electrical potential drop through the cascade. The configuration of this plane, designated the z plane, is shown in Fig. 1a. This particular potential flow through the cascade has no physical significance since the Kutta condition is not satisfied at the trailing edges of the blade profiles, but this potential flow may be used to effect the transformation of the cascade into the unit circle in the φ plane shown in Fig. 1b.

The correlation between the two planes is as shown in Fig. 1 with the shaded flow area between each pair of adjacent blades of the rectilinear cascade mapping into the entire flow area outside the circle. The points M_1 and M_2 are the points of maximum and minimum potential on the bodies in each of the planes and represent the stagnation points of the potential flow. With the knowledge that transformation between the two planes is possible and that the flow streamlines along the blade profiles correspond to the flow streamline along the circumference of the circle it may be seen that corresponding points on the bodies in each of the two planes must have the same fraction of the potential drop between M_1 and M_2 if conformality is to be preserved. Since values of the potential in each of the two planes are known, the point to point correspondence of the bodies bounded by their respective streamlines is established. While the analytical expression for the mapping function relating the two planes has not been determined, the information necessary to obtain the relationship between the velocities at any corresponding

point on the two bodies is obtainable and is invariant providing the geometry of the circle and cascade are not changed. The magnitude of the mapping derivative ($d\varphi/dz$), which establishes the relationship between the magnitude of the velocities in the two planes, is evaluated at each corresponding point by the quotient of the potential gradient ($d\phi/dz$) in the z plane and the potential gradient ($d\phi/d\varphi$) in the φ plane. The potential gradient in the z plane may be evaluated by graphical or other means from data taken from the electric analog while the potential gradient in the φ plane may be evaluated from the analytical expressions describing the potential distribution in the φ plane.

The flow about the circle in the φ plane may now be altered by the addition of vorticies to the sources and sinks. This alteration does not change the shape of the circle, but allows the Kutta condition to be satisfied by moving the rear stagnation point M_2 to a location coinciding with the trailing edge (T) and also allows any desired flow inlet angle to be specified for the cascade. The velocity distribution around the cascade blade profiles may now be determined using the previously determined value of the mapping derivative at each point. The equations necessary to perform the operation described here may be found summarized in a form suitable for calculations in Appendix A. The reader is referred to Ref. 2 for a complete exposition of the general method and Ref. 1 for a description of the techniques applicable to the utilization of the electric analog field plotter.

3.2 TRANSFORMATION BETWEEN CYLINDRICAL AND RECTILINEAR CASCADES

In order to utilize the electric analog described above it was necessary to transform the cylindrical cascade into a rectilinear cascade. If the cylindrical cascade exists in the complex w plane and the rectilinear cascade is desired in the complex z plane the relation to effect the conformal transformation of the w plane into the z plane is

$$z = \frac{sN}{2\pi} \log_e w$$

For a cylindrical cascade arranged for an outward radial flow this transformation has the effect of increasing the maximum camber and thickness of the blade profile. The details of this transformation may be found in Appendix C. The rectilinear cascade resulting from this transformation was used on the electric analog field plotter in the same manner as if it were a real cascade under investigation.

After determining the pressure distribution around the blade profiles of the rectilinear cascade it was necessary to transform the values obtained at each point on the rectilinear blade profile to the corresponding value on the cylindrical blade profile. This was accomplished using the inverse of the original transformation. The details of this transformation are shown in Appendix B.

3.3 EQUIPMENT

The item of equipment most essential to the electric analog field plotter is the conducting paper. This paper is marketed under the trade

name of "Teledeltos" paper. The working surface on which the paper was mounted is a plywood table surfaced with smooth tempered masonite. Two thin copper bus bars about five feet long are mounted near each edge of the table top. The bus bars are parallel and are 29.5 inches apart. A clamping arrangement is provided to clamp the conducting paper to the bus bars to insure a uniform electrical contact. A direct current voltage supply is used to provide the necessary electrical potential difference between the bus bars. The remaining items comprising the field plotter are the decade voltage divider, null meter, and probe which are used to make the necessary measurements. A list of equipment with specifications is given in Table I. The complete test setup is shown in Fig. 2 and shows the conducting paper clamped in place with the cascade cut out and the field plotter ready for measurements.

An additional item of equipment was the blade profile template used to guide the cutting knife when making the blade profile cutouts. The template was manufactured locally and was made of 0.125 inch flat stock tool steel. All specified blade profile dimensions were held to within $\pm$ 0.002 inch tolerances for a blade profile with a ten inch chord.

An item of equipment not directly associated with the field plotter was the CRC 102A Digital Computer. This computer is located in the Computation Center of the Department of Mathematics and Mechanics at the U. S. Naval Postgraduate School. The computer, while not a mandatory item in the development of the results of this investigation, saved considerable time and labor in the reduction of the data to the final form for presentation here.

3.4 PROCEDURE

The specifications of the cylindrical cascade to be investigated were obtained from Ref. 3 and are shown in Table II. The specifications included the blade profile coordinates (ξ_c, η_c), chord length (c), radius of the inner end of the chord reference line (r_i), and number of blades in the cascade (N). A cascade stagger angle (δ) of forty degrees was chosen for this investigation. The number of profile coordinates given proved inadequate to sufficiently define the transformed profile in the vicinity of the leading edge, therefore a very large scale drawing was made of the original airfoil to obtain additional coordinate points. The cylindrical cascade was then transformed into a rectilinear cascade using the relationships developed in Appendix C. The actual calculations were performed by the digital computer. The resulting coordinates of the transformed profile are shown in Table III as well as the rectilinear cascade stagger angle (ξ) and solidity (σ).

In laying out the rectilinear cascade on the field plotter it was necessary to maintain a reasonable distance from the leading and trailing edges of the cascade to the bus bars. It was also desirable to have blade profiles of large chord so that the data points could be accurately located. For these reasons a chord length of ten inches was chosen as the optimum chord for the rectilinear cascade layout. The blade profile template was made utilizing the coordinates listed in Table III converted to inches on the basis of a ten inch chord.

Prior to clamping the conducting paper to the table an approximate centerline was drawn down the length of the paper. The chord reference lines were constructed with the correct stagger angle and spacing using a drafting machine. The paper was then placed on the table and the previously drawn centerline was aligned with a line which had been marked on the working surface halfway between the fixed bus bars. The paper was then clamped to the bus bars in this position.

Before the cascade was cut from the paper an electrical potential difference was established between the bus bars and the paper was surveyed using the decade voltage divider, null meter, and probe. The purpose of this survey was to insure that the equipotential lines were approximately straight, parallel and very nearly equally spaced. Satisfaction of these conditions indicated that the paper had approximately uniform conductivity over its entire area. The electrical potential difference between bus bars was maintained at approximately 15 volts DC during all measurements. Since the use of the decade voltage divider and null meter allowed potential readings in terms of percent potential drop between the bus bars the maintenance of a uniform voltage was unnecessary.

The blade profiles were then carefully cut from the paper using the chord reference lines previously drawn as template locators. As shown in Fig. 2 the length of the bus bars was sufficiently long to allow a total of nine blade profiles to be cut from the paper.

One of the two interblade areas adjacent to the center blade was surveyed from one bus bar to the other and equipotential lines were

constructed at every ten percent potential drop near the bus bars and at every five percent potential drop in the cascade area. A streamline was constructed perpendicular to the equipotential lines starting at the "upstream" bus bar and continuing through the selected interblade area to the "downstream" bus bar. The ends of the paper were then trimmed along curves drawn parallel to the constructed streamline and located from that streamline by the appropriate number of blade spacings. The selected center interblade area was again surveyed, but no change in the center streamline was detectable. With the end conditions adjusted in this manner, the nine blade cascade then simulated a cascade of infinite extent.

Potential measurements on the upper and lower surface of the blade profiles were made at 36 chord stations on the three center blade cutouts. The three readings at each blade profile location were then averaged in an attempt to reduce the experimental error in the cascade layout and blade profile cutting procedure. The values of the maximum and minimum potential corresponding to the stagnation points were then determined. The potential at the trailing edge was determined by the mean value of 35 measurements taken, in groups of five each, at the trailing edges of the seven innermost blades of the cascade. The potential gradient near the bus bars ($\left[\frac{\Delta\phi}{\Delta x}\right]_{\infty}$) corresponding to the velocity perpendicular to the cascade axis at infinity (V_a) was taken as the mean value of a large number of measurements made near both bus bars.

In order to determine the potential gradient along the surface of the blade profiles using a graphical method, it was necessary to determine the arc length along the profile surface between data points. The arc length was determined from a scale drawing made of the profile with a 33 inch chord. The leading edge area was drawn to a scale of a 100 inch chord for these measurements. A very large scale graph of potential versus arc length was then made and a drafting machine protractor was used to measure the slope of the tangents at the data points. Because of the difficulties encountered in accurately measuring the slope of the potential curve a second method was also used to obtain the desired gradients. In this method the values of potential and arc length were entered into a digital computer program developed by Professor T. H. Gawain of the U. S. Naval Postgraduate School. This program fit a series of matched cubic curves to the measured potential points and calculated the slope of the fitted curve at each data point. The curves fitted to the experimental data points were adjusted so that the root mean square deviation of each curve was less than the estimated experimental uncertainty. The results of this curve fitting procedure were chosen as the final experimental values of potential and potential gradient at each data point. The data resulting from each of the two methods is presented for comparison in Tables IV and V.

Using the calculating procedure outlined in Appendix A the relation between the inlet, outlet, and mean vectorial flow angles (α_1, α_2', α_∞) was determined over a wide range of values using the digital

computer. The field plotter experimental data were then entered into the computing program with three inlet flow angles corresponding to the chosen inlet flow angles of the actual flow. The pressure coefficient (S) was calculated at each data point on the blade profile of the rectilinear cascade. The resulting pressure coefficients were then entered into the computer and a second program implementing the procedure outlined in Appendix B was used to convert these pressure coefficients into values appropriate to the cylindrical cascade. A graphic representation of the sequence of operations necessary to determine the pressure distribution resulting from an ideal flow through a cylindrical cascade is shown in Fig. 3.

3.5 RESULTS

The pressure distributions around the blade profiles of the cylindrical cascade as predicted by the potential flow solution are shown in Figs. 4, 5, and 6 for the inlet flow angles of 53, 48, and 58 degrees. The predicted relationship between the inlet flow angle, exit flow angle, and cascade turning angle ($\Delta\alpha$) is shown in Fig. 7.

The pressure distributions are presented in the form of the pressure coefficient S as a function of the distance along the blade chord. The pressure coefficient is defined as

$$S = \frac{p - p_2'}{\rho_2 V_2'^2}$$

where β_2' and V_2' refer to a hypothetical uniform flow at the radius of the trailing edges of the cylindrical cascade blades. In the radial flow field of the cylindrical cascade where the fluid undergoes constant diffusing action it is necessary to specify a radius in order to obtain invariant reference flow characteristics. This radius was chosen as the radius of the trailing edges of the blade profiles. Since flow conditions were not uniform at this radius the hypothetical reference flow conditions were obtained from the flow conditions at some larger, but finite, radius where mixing had been completed and the flow was actually uniform. The Laws of Continuity and Conservation of Momentum were satisfied in obtaining the hypothetical reference flow characteristics at the desired radius. The reference flow for the rectilinear cascade, which is normally the uniform flow far downstream of the cascade, was also transferred to the line of the trailing edges by continuity. Location of the reference flows in corresponding positions allowed the transformation of the rectilinear pressure coefficients to the values appropriate to the cylindrical cascade as outlined in Appendix B.

3.6 ACCURACY

The experimental uncertainty associated with the input values obtained from the electric analog field plotter and the effect of this uncertainty on the resulting flow angles and the pressure coefficient at a selected point is shown in Table VI. The pressure coefficient obtained from measurements at the 40 percent chord location on the upper surface of the blade profile of the rectilinear cascade has been chosen as a

representative value to demonstrate the effect of the input variations. The uncertainty intervals assigned to the various input quantities were either determined from a statistical analysis of a number of measurements or were estimated from a consideration of the influence of the various possibilities for experimental error. In addition to the uncertainty intervals determined for the results listed in Table VI it was found that the potential curve and its slope in the vicinity of the forward stagnation point on the field plotter could not be determined with sufficient accuracy to calculate reasonable values of the pressure coefficients in this area. This difficulty is indicated in the pressure maps of Figs. 4, 5, and 6 by the dotted curve in this area of uncertainty. This portion of each curve is unrelated to any calculated values.

4. THE ACTUAL FLOW

4.1 INTRODUCTION

The cylindrical cascade under investigation exists in the diffuser of a Compressor Test Rig located at the U. S. Naval Postgraduate School. This test rig is highly instrumented and was expressly designed as a research tool to further the understanding of the basic internal flow phenomena in turbomachines. The test rig is driven at 1800 RPM and requires about 15 horsepower to obtain a volumetric flow rate of about 90 to 140 cubic feet per second with a total pressure rise of about 12 to 8 inches of water, respectively. The Compressor Test Rig is described in detail in Ref. 3, and is pictured in Figs. 8 and 9.

The cascade consists of 42 equally spaced blades of NACA 4312 airfoil shape, 6.5 inch chord, and two inch width, arranged in the test rig as shown in Figs. 10 and 11. For this investigation the blades were positioned so that the chord reference line of each blade made an angle of 40 degrees with a radial line as shown in Fig. 11. Nine adjacent blades have static pressure taps located at the channel centerline. Each blade has a pattern of five taps distributed among the ten chordwise locations on the suction side and the five chordwise locations on the pressure side. Thus each set of three adjacent blades provides for 15 static pressure measurements around the airfoil. The nine instrumented blades provide for three static pressure measurements at each of the aforementioned 15 stations.

4.2 EQUIPMENT

A cylindrical probe was used to measure the cascade inlet angles (α_1), exit angles (α_3), and the total pressures at the cascade inlet and exit. This probe consists of a piece of one-fourth inch outside diameter stainless steel tubing with three 0.0135 inch diameter holes spaced 34.5 degrees apart in a plane perpendicular to the probe axis. The construction of the probe permits independent pressure connections to each of the three holes. The probe was mounted in an actuator as shown in Fig. 12. The actuator allowed the probe to be rotated about its axis or to be moved across the channel. The movement of the probe was controlled by a remote indicating control box. Once initial orientation of the probe and actuator assembly had been established, the position and angle of the probe relative to the actuator was always known.

A static tube was used to measure the static pressures at the cascade exit. The body of this tube consists of one-fourth inch outside diameter stainless steel tubing. The head of the tube consists of one-sixteenth inch outside diameter stainless steel tubing which is capped at the end with a hemispherical plug. About three-eights of an inch back from the tip of the head are four holes of 0.0145 inch diameter equally spaced around the circumference. The shape of the head is such that the holes lie on an extension of the axis of the body, so that when the tube is rotated the holes have negligible translation. The static tube was mounted in an actuator identical to the actuator used with the cylindrical probe, as shown in Fig. 12.

Two banks of water-filled manometers were used to determine blade static pressures. Three water-filled micromanometers were used to measure pressures which determined Test Rig volumetric flow rate, flow angles, and flow static and total pressures.

4.3 PROCEDURE

The cascade inlet angle was varied by throttling the airflow through the Test Rig. In essence this varied the radial velocity component and left the tangential velocity component practically unchanged. Test runs were performed at three inlet angles, 53, 48, and 58 degrees. These angles correspond to incidence angles of about 0, -5, and +5 degrees, respectively, where incidence angle (α_i) is defined as the angle between the inlet flow and the tangent to the camber line at the leading edge of the profile. To determine the inlet angle and inlet total pressure, the probe was inserted ahead of the cascade with the plane of the probe holes aligned with the channel centerline at a location as shown in Fig. 11. When the pressures obtained from the two outer holes were equal and the pressure obtained from the center hole was a maximum, the probe was known to be aligned with the direction of the flow, and the inlet total pressure and flow angle could be measured. A survey to determine inlet angle and total pressure variation across the diffuser channel was performed using four different flow rates.

To determine the cascade flow exit angles and total pressures the probe was positioned in the cascade wake as shown in Fig. 11. Since conditions in the wake varied in a circumferential direction, the plane

Two banks of water-filled manometers were used to determine blade static pressures. Three water-filled micromanometers were used to measure pressures which determined Test Rig volumetric flow rate, flow angles, and flow static and total pressures.

4.3 PROCEDURE

The cascade inlet angle was varied by throttling the airflow through the Test Rig. In essence this varied the radial velocity component and left the tangential velocity component practically unchanged. Test runs were performed at three inlet angles, 53, 48, and 58 degrees. These angles correspond to incidence angles of about 0, -5, and +5 degrees, respectively, where incidence angle (α_i) is defined as the angle between the inlet flow and the tangent to the camber line at the leading edge of the profile. To determine the inlet angle and inlet total pressure, the probe was inserted ahead of the cascade with the plane of the probe holes aligned with the channel centerline at a location as shown in Fig. 11. When the pressures obtained from the two outer holes were equal and the pressure obtained from the center hole was a maximum, the probe was known to be aligned with the direction of the flow, and the inlet total pressure and flow angle could be measured. A survey to determine inlet angle and total pressure variation across the diffuser channel was performed using four different flow rates.

To determine the cascade flow exit angles and total pressures the probe was positioned in the cascade wake as shown in Fig. 11. Since conditions in the wake varied in a circumferential direction, the plane

of the probe holes was aligned with the center of the diffuser channel and the probe was moved circumferentially through an angle corresponding to two blade intervals. To determine the cascade wake static pressures the static tube was positioned so that for each data point the holes of the static tube were in the same location as the center hole of the cylindrical probe had been. The static tube was aligned with the flow by utilizing the flow angle as previously determined by the cylindrical probe.

For each inlet angle, a survey of flow total pressure, static pressure, and flow angle was performed in the wake across the channel at a fixed circumferential location. At each inlet angle readings were taken of the static pressures on the blade surfaces.

4.4 RESULTS

Values of inlet flow total pressure and inlet angle are plotted versus channel width in Fig. 13. Values of wake flow total pressure and wake flow angle are plotted versus channel width for a fixed circumferential location in Fig. 14. Values of wake flow total pressure, static pressure, and angle are plotted versus blade spacing for the inlet flow angles of 53, 48, and 58 degrees in Figs. 15, 16, and 17. Pressure coefficients for the three specified inlet angles are plotted versus chord in Figs. 4, 5, and 6. All measurements except cross channel surveys were made at points in a plane midway between the two diffuser channel walls, and the flow determined from these measurements was considered to be a two-dimensional flow existing in that plane.

To determine pressure coefficients that can be compared to those obtained from the ideal flow, a common reference must be used. This reference was fixed as a uniform flow existing at the trailing edge radius, as described in Section 3.5. Since uniform conditions do not exist at the radius of the trailing edge, the reference uniform flow had to be determined in a logical manner from the knowledge of the existing flow.

The actual flow was determined from data taken along the wake flow survey arc as shown in Figs. 10 and 11. A uniform flow occurring at the same radius was then described that had the same mass flow rate and the same tangential momentum flow as the actual flow. The uniform flow was then described as it would occur at the trailing edge radius, and as such was used as the reference flow. The method used in determining this reference flow is described in Appendix D.

4.5 ACCURACY

The flow angles as measured by the cylindrical probe, actuator, and micromanometer system, are estimated to be in error not more than one degree. The error in probe-actuator orientation and actuator installation is probably not more than one-half degree and the remaining error is probably not more than one-half degree since flow angle measurements were duplicated with consistently less than one-half degree variation.

The flow total pressures, as measured by the same system, are estimated to be correct within five hundredths of an inch of water. Most of this error is accounted for by a small, slow aperiodic fluctuation of the total pressure.

The flow static pressures as measured by the static probe, actuator, and micromanometer system, are estimated to be correct within five hundredths of an inch of water. The static pressure also exhibited the same fluctuation as the total pressure.

The blade static pressures are estimated to have an error of not more than one millimeter of water due to manometer reading error. An additional variation in readings at identical locations of the blades was present since three blades were used to obtain the static pressure at each location and the actual flow was not identical around all nine instrumented blades.

The accuracy of the value of the reference static and dynamic pressure is primarily dependent upon the accuracy of the measurements of the actual flow, since the analytical and graphical operations performed upon the measured flow have a less significant effect on the resulting reference pressures than do the original measurements.

The estimated error in pressure coefficient due to the estimated error in each of the aforementioned parameters would be extremely difficult to accurately determine. If the error in the pressure coefficient due to the estimated error of one degree in inlet angle were desired, an additional set of experimental readings would have to be made with the inlet angle varied by one degree. But inherent to these results would be the error in determining the flow angle, in addition to all the other experimental errors present.

5. DISCUSSION

5.1 COMPARISON OF THE IDEAL AND ACTUAL FLOW RESULTS

As shown in the pressure maps of Figs. 4, 5, and 6, the magnitude of the pressure coefficient at a given point as predicted by the ideal flow conditions through the cascade has very little correlation with the magnitude resulting from measurements of the actual air flow through the cascade. It is interesting to note, however, that the pressure maps for the ideal and actual flow conditions exhibit a very good similarity in terms of shape. The exception to this similarity occurs at the peak negative pressure on the suction side of the cascade blade at inlet angles of 53 and 58 degrees. The actual flow conditions did not produce a pressure peak as predicted by the ideal flow. The failure to obtain a pressure peak under actual flow conditions similar to that predicted by the ideal flow may be the result of local flow separations due to the viscosity of the air and may possibly be due to the variations in the flow conditions across the blade width as discussed in Section 5.2.

The integrated area of the pressure maps represents a non-dimensional force coefficient which, in general, is a measure of the force exerted on the fluid by each cascade blade. It may be seen from Figs. 4, 5, and 6 that the cascade under actual flow conditions was much less effective in exerting the forces necessary to alter the fluid flow direction than was predicted by the ideal flow calculations. This reduced effectiveness at all inlet angles is also shown in Fig. 7 in terms of a smaller cascade turning angle obtained in the actual flow

5. DISCUSSION

5.1 COMPARISON OF THE IDEAL AND ACTUAL FLOW RESULTS

As shown in the pressure maps of Figs. 4, 5, and 6, the magnitude of the pressure coefficient at a given point as predicted by the ideal flow conditions through the cascade has very little correlation with the magnitude resulting from measurements of the actual air flow through the cascade. It is interesting to note, however, that the pressure maps for the ideal and actual flow conditions exhibit a very good similarity in terms of shape. The exception to this similarity occurs at the peak negative pressure on the suction side of the cascade blade at inlet angles of 53 and 58 degrees. The actual flow conditions did not produce a pressure peak as predicted by the ideal flow. The failure to obtain a pressure peak under actual flow conditions similar to that predicted by the ideal flow may be the result of local flow separations due to the viscosity of the air and may possibly be due to the variations in the flow conditions across the blade width as discussed in Section 5.2.

The integrated area of the pressure maps represents a non-dimensional force coefficient which, in general, is a measure of the force exerted on the fluid by each cascade blade. It may be seen from Figs. 4, 5, and 6 that the cascade under actual flow conditions was much less effective in exerting the forces necessary to alter the fluid flow direction than was predicted by the ideal flow calculations. This reduced effectiveness at all inlet angles is also shown in Fig. 7 in terms of a smaller cascade turning angle obtained in the actual flow

From a very general consideration of the influence of the variation of the above parameters on the values of the pressure coefficient, and from the comparison of the three measurements made at each location on the blade profiles, it is concluded that the maximum probable error in pressure coefficient is not more than plus or minus 0.25.

than was predicted by the ideal flow. It is also shown in Fig. 7 that the nearly constant cascade exit angle predicted by the ideal flow calculations was not attained under actual flow conditions even though the cascade was tested over a small range of low incidence angles. With the exception of the prediction of the general shape of the pressure maps, which is of little value, the attempt to predict the performance of the cascade under actual operating conditions was unsuccessful. Various possible reasons for this failure are discussed in Section 5.2.

5.2 DEVIATION OF THE ACTUAL FLOW FROM POTENTIAL FLOW REQUIREMENTS

The actual flow does not meet many of the conditions necessary for the potential flow of an ideal fluid as set forth in Section 3.1. These conditions will be discussed individually in the following paragraphs, including an estimation of the effect of each condition upon the difference between the results for the ideal and actual flows.

The actual flow is not inviscid, and as such is subject to total pressure losses resulting from viscosity. These losses will be greater for the cylindrical cascade than would be the losses for a comparable rectilinear cascade, since boundary layer growth is more rapid in a diffuser than in a constant area channel due to the decelerating nature of a flow in a diffuser. As stated in Ref. 2, for rectilinear cascades good correlation of cascade pressure maps and turning angles has been obtained when comparing ideal flows as determined by an electrical analog field plotter with actual flows as determined by cascade tests. Even

with the increased effect of viscosity because of the diffusing flow, it is concluded that viscous effects constitute but a very small portion of the difference between the results for the ideal and actual flows in the cascade under investigation.

The actual flow is not irrotational. It can be shown that energy cannot be added to an irrotational real fluid by means of a rotor without the fluid becoming rotational, thus in the Compressor Test Rig the air is rotational when it approaches the diffuser cascade. The effect of the rotationality of the actual flow upon the difference between the results for the ideal and actual flow is not known, but it is believed to be of secondary importance.

The actual flow is non-steady. The rotor consists of 23 blades, and turns at 1800 RPM, therefore the actual flow "pulses" about 690 times per second. Due to the damping effect of the viscosity of the actual flow, and because all measurements made of the actual flow properties were time-averaged measurements, the effect of the non-steady condition of the actual flow upon the difference of the results for the ideal and actual flow is considered negligible.

The actual flow is not incompressible. As discussed in Ref. 3, however, the density of the actual flow does not vary more than two percent. Therefore the effect of the compressibility of the actual flow upon the difference between the results for the ideal and actual flow is considered negligible.

The actual flow is not two-dimensional. As shown in Figs. 13 and 14, total pressures and flow angles vary considerably across the width of the diffuser channel ahead of and behind the cascade. A comparison of Figs. 13a and 14a shows that, with flow static pressure remaining about constant across the channel width, at all flow rates the maximum flow velocity occurs at about 0.25 channel width at the cascade inlet and at about 0.50 channel width at a fixed circumferential location in the cascade exit. The variation in the location of the peaks and in the general shape of the total pressure curves between Figs. 13a and 14a proves that the flow in the plane of the blade measurements (channel width = 0.50) is not a two-dimensional flow and that cross-flow velocities do exist between the cascade inlet and exit stations. The existence of cross-flow velocities on the blades is evident by noting in Fig. 13b that the inlet angle can vary across the width of the blade by as much as 30 degrees. If the "center" of the blade were operating at zero degrees angle of incidence, one portion of the blade less than one inch distant in a spanwise direction could be operating at an incidence angle of -10 degrees and another portion of the blade also less than one inch distant in a spanwise direction could be operating at an incidence angle of +20 degrees. Pressure maps are shown for the "center" of the blade operating at 0, -5, and +5 degrees angle of incidence in Figs. 4, 5, and 6, and the variation of these maps gives some indication of the variation of the static pressure on the blade in the spanwise direction across the channel width. With cascade inlet angles of 53 and

48 degrees, the pressure at the peaks of the total pressure curves of Figs. 15 and 16 is greater than the total pressure at the cascade inlet. Since no energy is added to the actual flow in the diffuser section, the total pressure of a two-dimensional flow must decrease and cannot increase at any circumferential location in the wake. This increase of total pressure is indicative of the existence of cross-flow velocities and indicative that the fluid whose properties were measured at the cascade exit was not the same fluid whose properties were measured at the cascade inlet. From the above considerations it is concluded that the three-dimensional characteristics of the actual flow are predominant in causing the difference between the results for the ideal and actual flow.

No cascade can operate effectively over a range in incidence angle much greater than -7 to +7 degrees. Since the diffuser cascade is operating at simultaneous incidence angles that vary as much as 30 degrees, it is obvious that the losses in the cascade are excessive. It is therefore recommended that a new rotor be built for the Compressor Test Rig and its design should be governed by the aim of increasing the uniformity of the flow ahead of the diffuser cascade without materially increasing the losses associated with the rotor itself.

Additional investigations of cylindrical cascade performance in actual flows should be made with potential flow conditions more nearly satisfied. The first investigation could be made using the cylindrical cascade formed by the inlet guide vanes of the Compressor Test Rig. The actual flow through the inlet cascade would be steady, irrotational,

and very nearly two-dimensional. With these potential flow conditions satisfied, correlation between the results for the ideal and actual flows should be good.

Of more interest, however, would be an investigation of the actual flow in a diffusing cylindrical cascade with the same flow conditions as specified for the inlet cascade. If good correlation is obtained between the results for the ideal and actual flow in this diffusing cylindrical cascade, then the cylindrical cascade in the diffuser of the Compressor Test Rig could be investigated again using the redesigned rotor previously discussed.

5.3 THE ELECTRIC ANALOG METHOD

As is indicated in the discussion above, it is felt that the failure of this investigation to obtain reasonably correct predictions of cylindrical cascade performance under actual operating conditions resulted from violations by the actual flow of the requirements of the ideal flow, and not as a result of any gross inaccuracies in the potential flow solution. It is felt that the potential flow solution which was obtained is reasonably accurate.

The analysis of the sensitivity of the results to variations in the measured quantities, as shown in Table VI, reaffirms the statement contained in Ref. 1 that a high order of precision is desirable in measuring the electrical potential at the profile trailing edge point. An indirect method of obtaining this value, utilizing the potential flow about a wedge, was proposed by Fahland and Hawkins in Ref. 1. This method

was attempted in this investigation, but resulted in an impossible value of the trailing edge potential and was therefore discarded. The use of a large number of measurements as described in Section 3.4 is not proposed as a superior method, but was used in an attempt to reduce the uncertainty associated with this critical value. The numerous measurements at the trailing edge point are not properly independent since the location of the probe tends to become "grooved" by the small hole in the conducting paper resulting from the first measurement and enlarged by succeeding measurements at the same point. If the probe is improperly located during the first measurement all succeeding measurements also tend to be improperly located. The destructive nature of the first measurement is the second cause for error in this method in that it slightly alters the potential field in the vicinity of the trailing edge and destroys the original potential value there. Ideally all potential values should be obtained by a single measurement at each point. An improved version of the indirect method proposed in Ref. 1 would be desirable and would be effective in improving the reliability of the results.

The authors of Ref. 1 proposed two methods of obtaining the potential gradient along the surface of the blade profiles, direct measurement and graphical. The direct measurement method approximates the potential gradient by measurement of the potential drop over very small distances along the blade profile using a double probe and a precision potentiometer. Both Ref. 1 and Ref. 2 indicate that satisfactory results may be obtained using the direct measurement method. In the present investigation the

direct measurement method was attempted, but was discarded when it was discovered that this method resulted in an experimental uncertainty which was unacceptable. Using the direct measurement method, difficulty was encountered in obtaining uniform contact between each prong of the double probe and the conducting paper. It is also felt that erroneous potential differences were measured due to extraneous potentials introduced in the potentiometer circuit by the contact of dissimilar conductors in that circuit. An additional error may have been introduced by the very small residual current (resulting from imperfect balance of the potentiometer circuit) which established a current source-sink effect in the vicinity of the probe. Because of the unacceptable experimental uncertainty of the direct measurement method a graphical method coupled with a curve fitting technique was used in this investigation.

A third departure from the procedures for utilizing the electric analog field plotter as recommended in Ref. 1 was made in the use of a straight flat table rather than the folding table devised by the authors of Ref. 1. The folding table eliminates the necessity for adjusting the end conditions of the paper to simulate a cascade of infinite extent. With a cascade of high solidity, such as was studied in this investigation, the flat table field plotter can accommodate a sufficient number of profiles so that the area near the center profile is quite insensitive to small errors in the end conditions. For cascades of lower solidity an increase in the usable length of the flat table to obtain a similar insensitivity of the center area to the end conditions should be considered. The

modification requires only that the length of the bus bars and table be increased to accommodate a suitably large number of blades. It is felt that this simple modification would be justified in order to avoid the much more complex folding table arrangement.

In general, it is felt that all measurement techniques, instruments, and data processing procedures employed in this investigation are consistent with the uniformity specified for the specific resistance of the conducting paper. An improved conducting medium, recommended in Ref. 1, would require improvement in instrument sensitivity and accuracy of data point location when making measurements.

Reasonable values for the pressure coefficient at points near the stagnation point M_1 on the blade profile in the potential flow of the electric field plotter could not be obtained. This failure to obtain reasonable values is a direct result of the high solidity and large maximum blade profile thickness of the rectilinear cascade which was obtained by transformation of the cylindrical cascade under investigation. This high solidity and large maximum profile thickness have a direct effect on the configuration of the ζ plane. An increase in both parameters tends to bring the sources and sinks on the real axis closer to the unit circle by reducing the quantity b to values very close to unity. The solidity of the rectilinear cascade studied in this investigation was 1.804 while the maximum blade profile thickness was 12.7 percent chord. This cascade configuration resulted in a value of b equal to 1.035 as compared to the circle radius of unity. This close proximity of the sources and

sinks to the unit circle in the vicinity of M_1 and M_2 in the φ plane makes the determination of the location of corresponding points and the mapping derivative very sensitive to experimental uncertainties of the measured values of potential and potential gradient in the z plane near M_1 and M_2. This sensitivity to experimental error would be increased if rectilinear cascades with combinations of solidity and maximum profile thickness greater than those used in this investigation were studied using the electric analog method. This difficulty is inherent to any conformal transformation method which maps a rectilinear cascade of infinite extent into a single closed curve.

6. CONCLUSIONS

It is concluded that the performance of the cylindrical cascade in the diffuser of the Compressor Test Rig could not be predicted by the two-dimensional solution of the flow of an ideal fluid through the cascade. It is further concluded that the actual flow conditions through the cylindrical cascade are at such a great variance with the two-dimensional flow requirement that no accurate prediction of the performance of this cascade can be made using the electrical analog-conformal mapping method.

7. REFERENCES AND BIBLIOGRAPHY

Ref. 1: Fahland, F. R. and L. H. Hawkins. "An Electrical Analogy for Analysis of Flow Through Cascades." U. S. Naval Postgraduate School, 1958

Ref. 2: Vavra, M. H. Aero-Thermodynamics and Flow in Turbomachines. New York: John Wiley & Sons, Inc., 1960

Ref. 3: Vavra, M. H. and T. H. Gawain. "Compressor Test Rig for Investigation of Flow Phenomena in Turbomachines." U. S. Naval Postgraduate School, 1955

Bibliography of material used as background but not referred to specifically in the text.

Carter, A. D. S. "Some Tests on Compressor Cascades of Related Airfoils having Different Position of Maximum Camber." Aeronautical Research Council R. & M. No. 2694, 1953

Garrick, I. E. "On the Plane Potential Flow Past a Lattice of Arbitrary Airfoils." NACA Report No. 788, Washington, D.C., 1944

de Haller, P. "Application of Electrical Analogy to the Investigation of Cascades." Extract from Proceedings of the Sixth International Congress of Applied Mathematics, Paris, 1946. Sulzer Technical Review, No. 3/4, pp 11-17, 1947

Shepherd, D. G. Principles of Turbomachinery. New York: The MacMillan Company, 1956

TABLE I

LIST OF EQUIPMENT

1. Conducting Paper	- Teledeltos Paper, Type "L", Sunshine Scientific Instrument Co., Specific Resistance approximately 4000 ohms with tolerances of ± 3% along length and ± 8% across width of paper, rolls are 20 feet long and 34 inches wide.
2. Potential Supply	- Heathkit Battery Eliminator, Model BE-4.
3. Null Meter	- General Electric DC Micro Ammeter, Type DO-71, Model A29AA1, coil resistance of 1700 ohms, detecting sensitivity power on the order of eight micro-micro watts.
4. Voltage Divider	- Electro-Measurements Inc. Dekavider, Model RV622, linearity of ± 0.0025%, input resistance of 10,000 ohms, Serial 13,049.
5. Probe Actuators	- Two BBM 5180 5" Traverse Miniature Actuators, 180 degree angular motion, L. C. Smith & Co.
6. Remote Indicating Control Box	- Indication Automatic Balance, Potentiometer bridge balance type, ABI-3, L. C. Smith & Co.
7. Cylindrical Probe	- Fabricated locally from one-fourth inch outside diameter stainless steel tubing, 16 inches in length.
8. Static Tube	- Fabricated locally. Body made from one-fourth inch outside diameter stainless steel tubing 14 inches long, head made of one-sixteenth inch outside diameter stainless steel tubing.
9. Micromanometers	- Meriam Instrument Co., Model A-750, measures pressures to an accuracy of 0.001 inch of water pressure.

10. Manometer Bank - Wind Tunnel Instrument Co., 40 tubes of 250 centimeter capacity, smallest gradations one-fifth centimeter.

11. Manometer Bank - Twenty tubes of 13 inch capacity. Smallest gradations one-tenth inch.

TABLE II

SPECIFICATIONS FOR CYLINDRICAL CASCADE

δ = 40 degrees c = 6.5 inches
N = 42 r_1 = 21.5 inches

Coordinates for NACA 4312 Profile

(Stations and ordinates in percent of profile chord)

Upper Surface		Lower Surface	
Station	Ordinate	Station	Ordinate
0	0.80	0	0
1.25	2.65	1.25	-1.29
2.50	3.63	2.50	-1.75
5.00	5.11	5.00	-2.19
7.50	6.23	7.50	-2.34
10.00	7.13	10.00	-2.39
15.00	8.47	15.00	-2.31
20.00	9.36	20.00	-2.17
25.00	9.83	25.00	-2.08
30.00	10.00	30.00	-2.00
40.00	9.75	40.00	-1.88
50.00	9.00	50.00	-1.62
60.00	7.86	60.00	-1.28
70.00	6.40	70.00	-0.95
80.00	4.63	80.00	-0.65
90.00	2.54	90.00	-0.39
95.00	1.39	95.00	-0.25
100	0	100	0

The leading edge is a portion of the circle of radius 1.61 percent chord with center located at station 1.56 percent chord and ordinate 0.41 percent chord.

TABLE III

SPECIFICATIONS FOR RECTILINEAR CASCADE

ξ = 35.4 degrees σ = 1.804

Coordinates for transformed Profile

(Stations and ordinates in percent of profile chord)

Upper Surface		Lower Surface	
Station	Ordinate	Station	Ordinate
0	1.18	0	0
1.25	3.13	1.25	-1.21
2.50	4.26	2.50	-1.65
5.00	6.00	5.00	-1.93
7.50	7.31	7.50	-1.96
10.00	8.35	10.00	-1.90
15.00	10.02	15.00	-1.50
20.00	11.18	20.00	-1.10
25.00	11.86	25.00	-0.75
30.00	12.22	30.00	-0.45
40.00	12.11	40.00	-0.07
50.00	11.31	50.00	+0.23
60.00	9.93	60.00	0.56
70.00	8.21	70.00	0.68
80.00	5.95	80.00	0.55
90.00	3.25	90.00	0.30
95.00	1.75	95.00	0.09
100	0	100	0

The leading edge is a portion of the circle of radius 1.80 percent chord with center located at station 1.70 percent chord and ordinate 0.60 percent chord.

TABLE IV

VALUES OF POTENTIAL ON THE BLADE PROFILE FROM THE FIELD PLOTTER AND MODIFIED VALUES RESULTING FROM CURVE FITTING

	Data measured from Field Plotter		Data as modified by curve fitting	
Chord Station	Upper Surface Potential	Lower Surface Potential	Upper Surface Potential	Lower Surface Potential
0	68.29	----	68.29	----
0.25	68.70	66.52	68.72	66.55
0.50	69.00	66.04	68.98	66.10
1.00	69.28	65.42	69.27	65.41
2.00	69.56	64.31	69.58	64.29
3.00	69.74	63.38	69.75	63.35
4.00	69.80	62.54	69.80	62.54
5.00	69.81	61.81	69.80	61.80
7.00	69.68	60.46	69.67	60.49
9.00	69.42	59.28	69.42	59.28
11.00	69.06	58.15	69.07	58.15
13.00	68.64	57.09	68.64	57.08
15.00	68.14	56.04	68.13	56.04
17.50	67.40	54.77	67.41	54.78
20.00	66.60	53.57	66.59	53.57
25.00	64.74	51.31	64.74	51.31
30.00	62.70	49.20	62.69	49.20
35.00	60.46	47.12	60.43	47.13
40.00	58.03	45.11	58.09	45.14
45.00	55.73	43.20	55.71	43.20
50.00	53.33	41.34	53.32	41.33
55.00	50.98	39.56	50.95	39.56
60.00	48.59	37.87	48.63	37.88
65.00	46.36	36.30	46.36	36.29
70.00	44.08	34.78	44.12	34.79
75.00	41.90	33.37	41.89	33.37
80.00	39.70	32.05	39.67	32.06
85.00	37.43	30.87	37.43	30.86
90.00	35.16	29.84	35.16	29.84
95.00	32.85	29.09	32.85	29.09
100	29.48	29.48	29.44	29.44

Chord stations are given in percent chord. Potential values are given in percent potential difference between bus bars. The modified value of potential at the trailing edge is the mean value of 35 measurements.

TABLE V

VALUES OF POTENTIAL GRADIENT ON THE BLADE PROFILE DERIVED FROM MEASUREMENTS ON THE FIELD PLOTTER AND MODIFIED VALUES RESULTING FROM CURVE FITTING

	Data determined from Field Plotter measurements		Data as modified by curve fitting	
Chord Station	Upper Surface Potential Gradient	Lower Surface Potential Gradient	Upper Surface Potential Gradient	Lower Surface Potential Gradient
0	0.6873	----	0.6960	----
0.25	.5243	1.2348	.5537	1.2040
0.50	.4681	1.1369	.4605	1.1509
1.00	.3378	1.0446	.3438	1.0696
2.00	.1853	0.9110	.1913	0.9398
3.00	.0992	.8243	.0747	.8371
4.00	.0320	.7581	.0172	.7568
5.00	.0223	.6959	.0206	.6951
7.00	.0919	.6371	.0861	.6203
9.00	.1331	.5658	.1392	.5702
11.00	.1823	.5336	.1847	.5358
13.00	.2263	.5132	.2229	.5173
15.00	.2648	.4895	.2563	.5048
17.50	.3010	.4806	.2978	.4859
20.00	.3346	.4734	.3373	.4633
25.00	.3772	.4296	.3802	.4258
30.00	.4348	.4091	.4321	.4088
35.00	.4628	.3990	.4572	.3959
40.00	.4663	.3839	.4674	.3903
45.00	.4628	.3706	.4711	.3778
50.00	.4628	.3541	.4689	.3598
55.00	.4628	.3443	.4611	.3418
60.00	.4487	.3153	.4494	.3244
65.00	.4400	.3010	.4403	.3073
70.00	.4296	.2883	.4340	.2904
75.00	.4193	.2695	.4307	.2723
80.00	.4400	.2509	.4302	.2505
85.00	.4348	.2126	.4326	.2237
90.00	.4348	.1838	.4379	.1797
95.00	.4505	.1007	.4462	.1156

Chord stations are given in percent chord. Values of potential gradient are given in percent potential difference between bus bars per percent chord.

TABLE VI

EFFECT OF EXPERIMENTAL UNCERTAINTY OF MEASUREMENTS MADE ON FIELD PLOTTER UPON TURNING ANGLES AND PRESSURE COEFFICIENTS OF IDEAL FLOW THROUGH THE CYLINDRICAL CASCADE

Quantity	Value	Estimated Experimental Uncertainty	Variation of Pressure Coefficient Value	Variation of Turning Angle Value
V_a	2.85	$\pm$ 0.04	$1.749^{+ .048}_{- .046}$	$26.65^{+ 0.25}_{- 0.16}$
ϕ_1	69.80	$\pm$ 0.01	$1.749^{+ .001}_{- .002}$	$26.65^{+ 0.02}_{- 0.02}$
ϕ_2	28.85	$\pm$ 0.01	$1.749^{+ .013}_{- .014}$	$26.65^{+ 0.34}_{- 0.36}$
ϕ_T	29.44	$\pm$ 0.05	$1.749^{+ .068}_{- .066}$	$26.65^{+ 1.70}_{- 1.64}$
ϕ	58.09	$\pm$ 0.02	$1.749^{+ .002}_{- .003}$	26.65 ± 0
$\frac{d\phi}{dz}$	0.4674	$\pm$ 0.0015	$1.749^{+ .018}_{- .018}$	26.65 ± 0

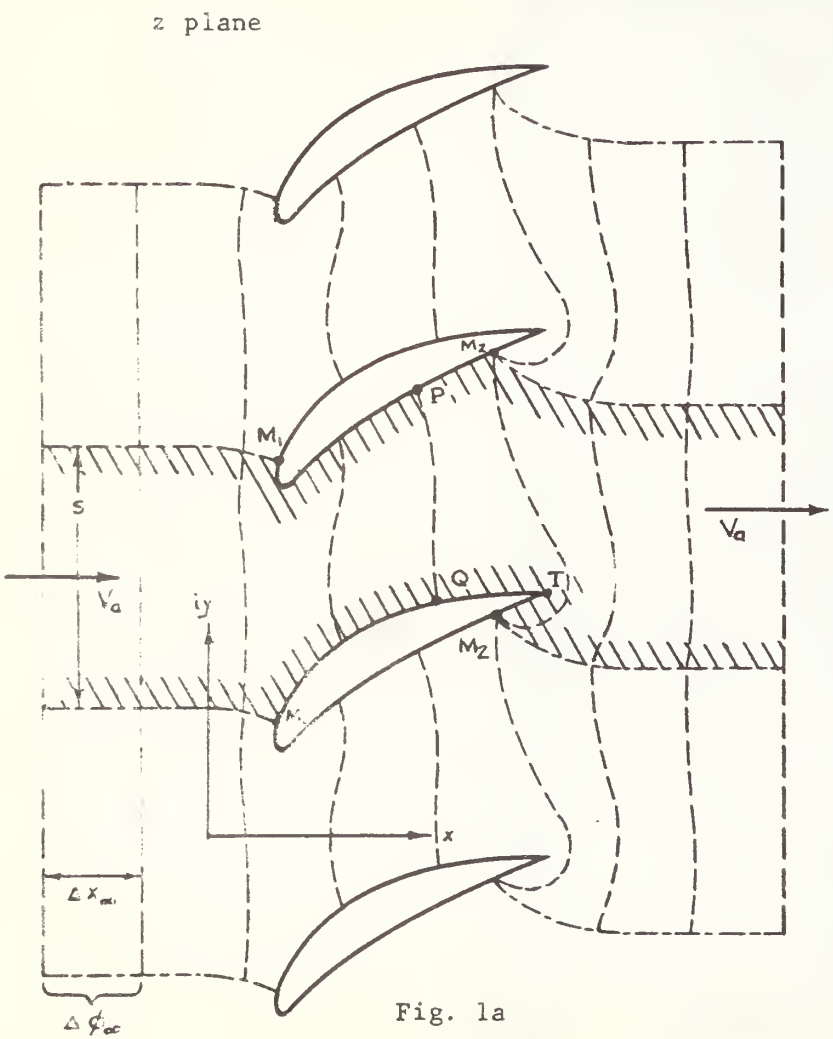

Fig. 1a

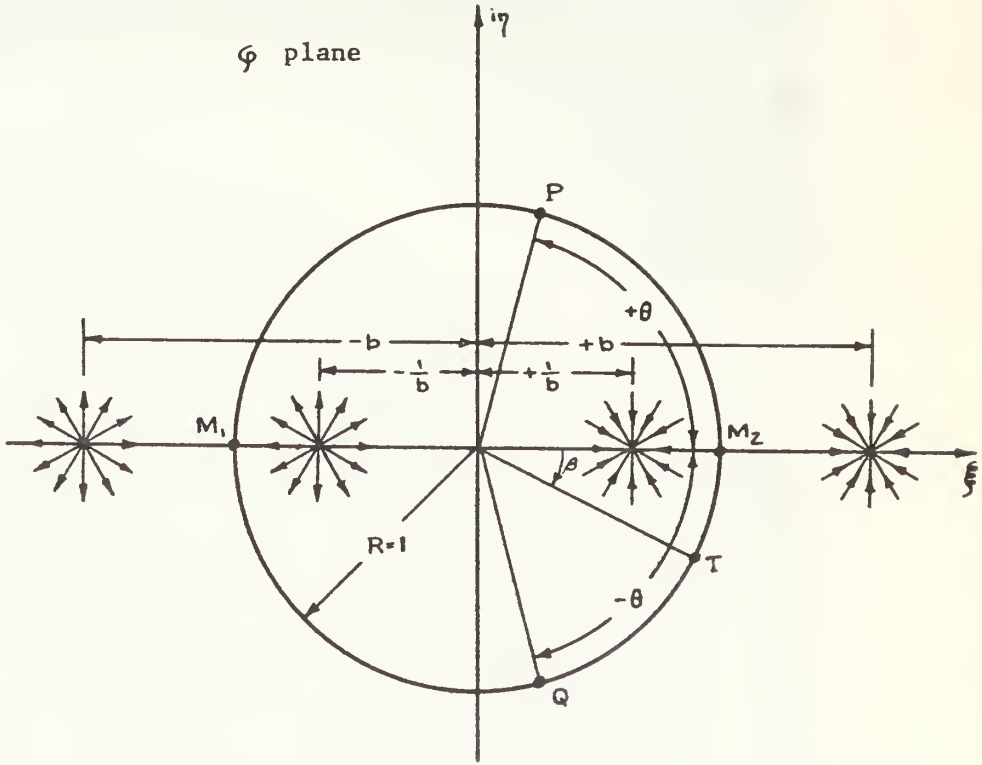

Fig. 1b

Fig. 1

Conformal Transformation of a Rectilinear Cascade into a Circle

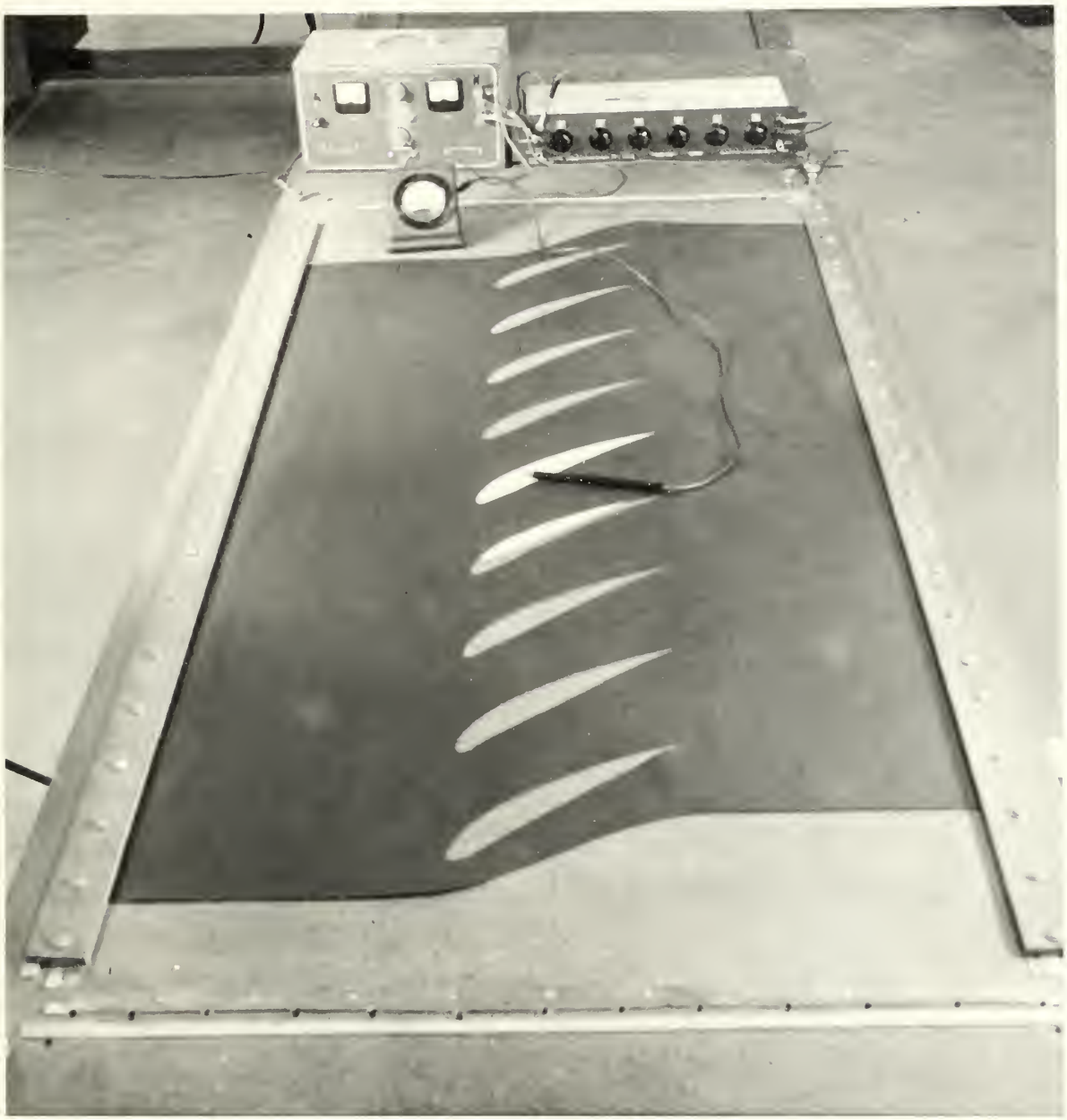

Fig. 2

The Electric Analog Field Plotter

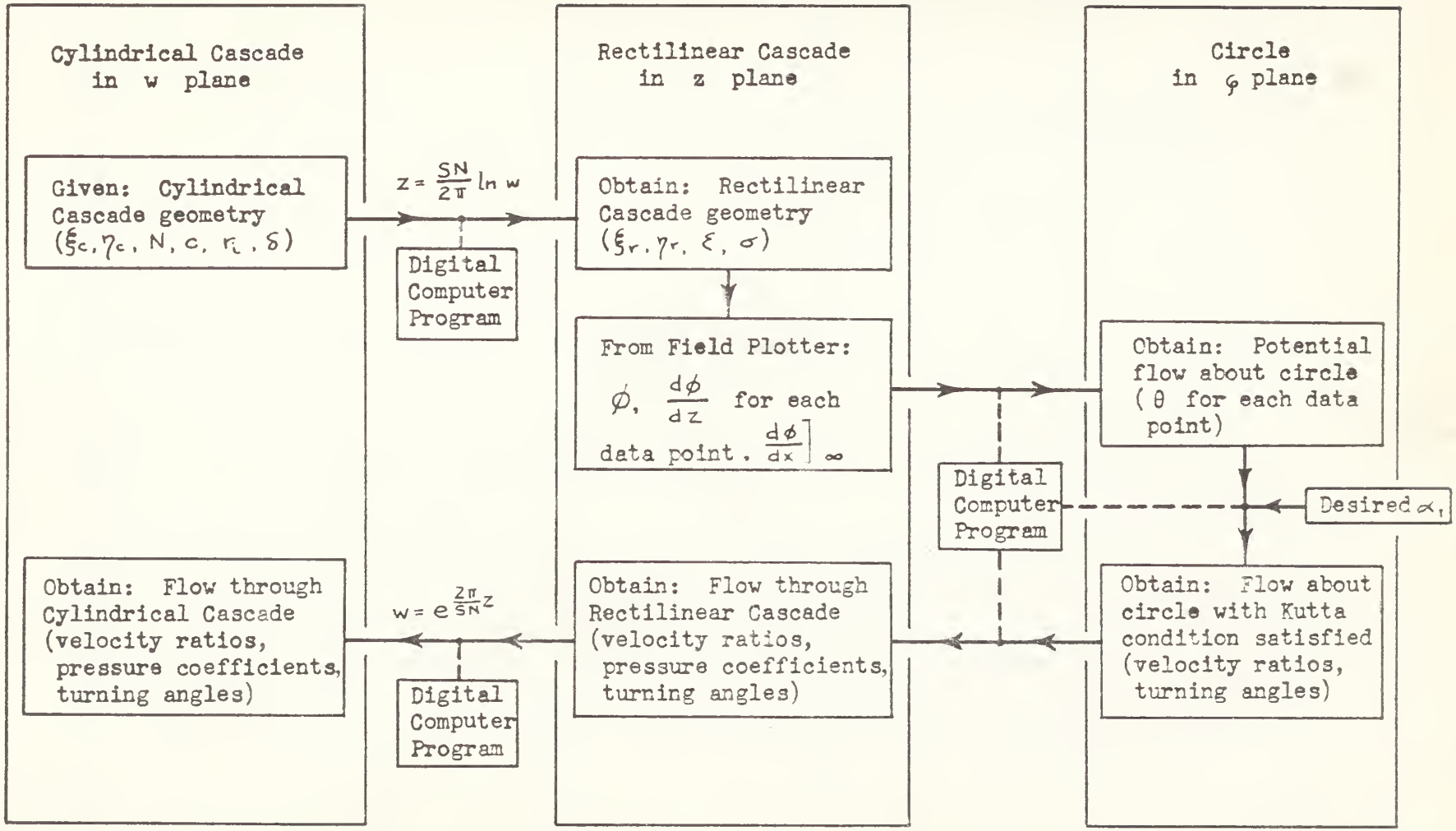

Fig. 3

Sequence of Operations to Determine Ideal Flow through a Cylindrical Cascade

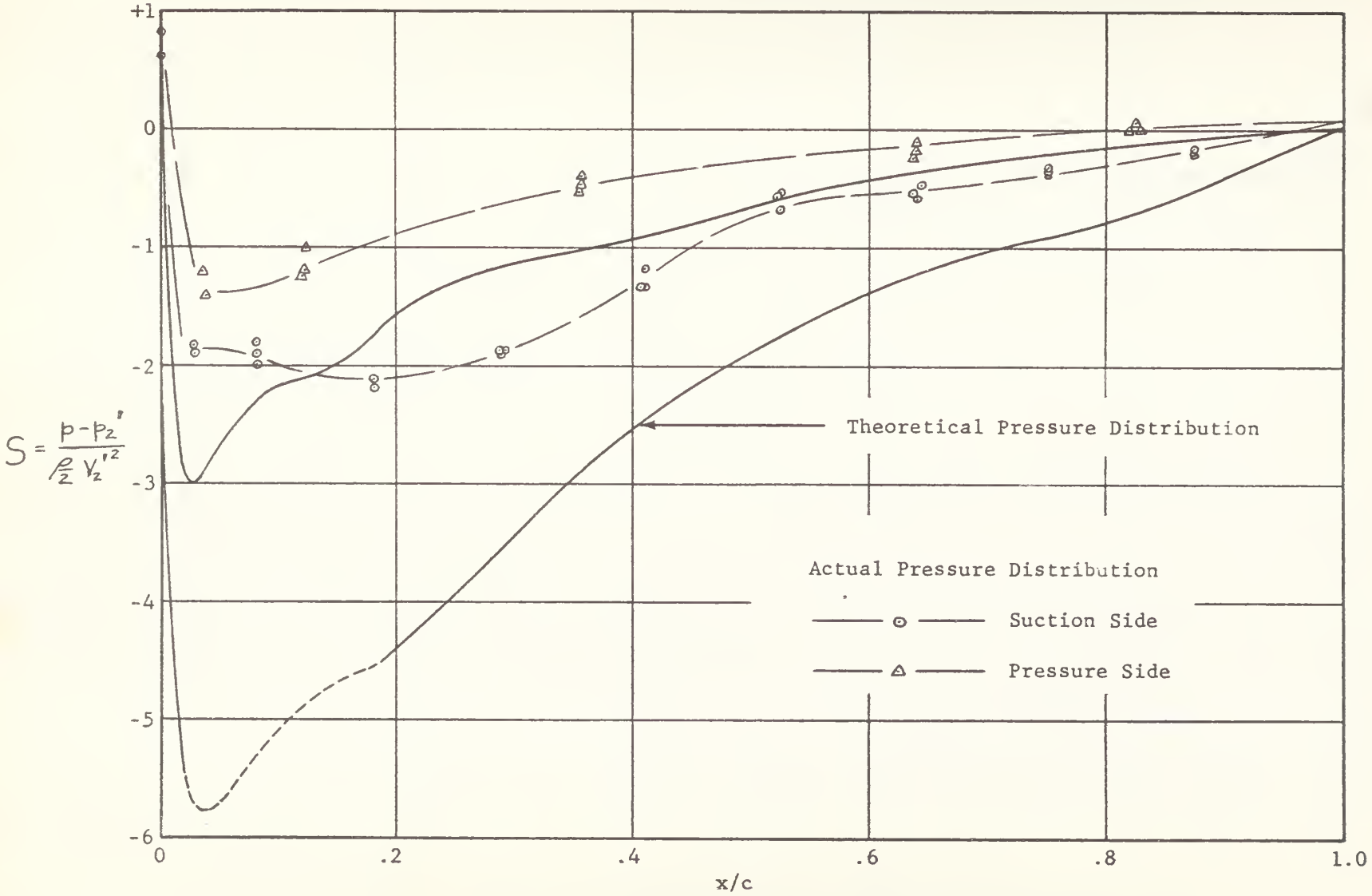

Fig. 4 Pressure Distribution around Blade Profiles for Ideal and Actual Flows with an Inlet Flow Angle of 53 degrees

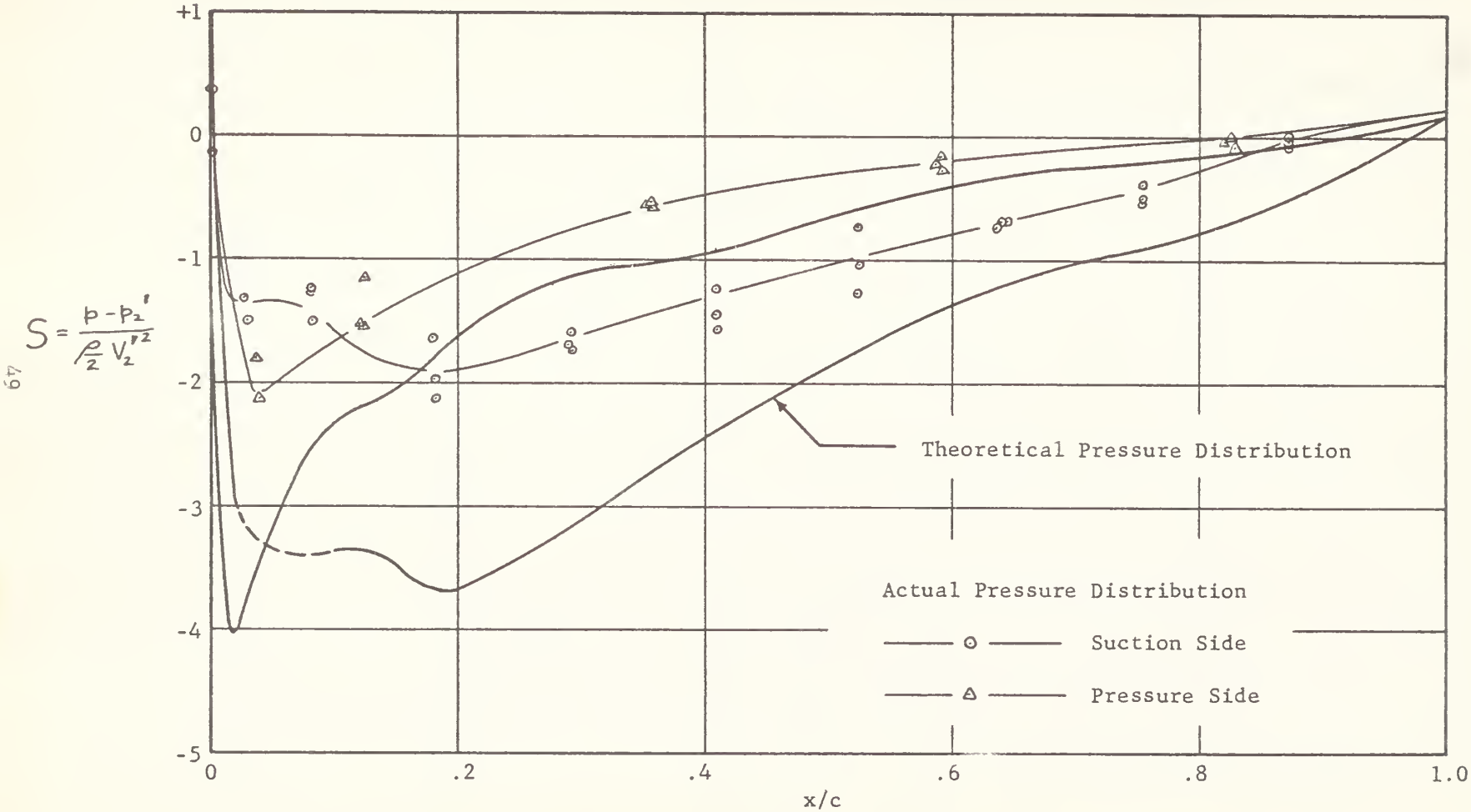

Fig. 5 Pressure Distribution around Blade Profiles for Ideal and Actual Flows with an Inlet Flow Angle of 48 degrees

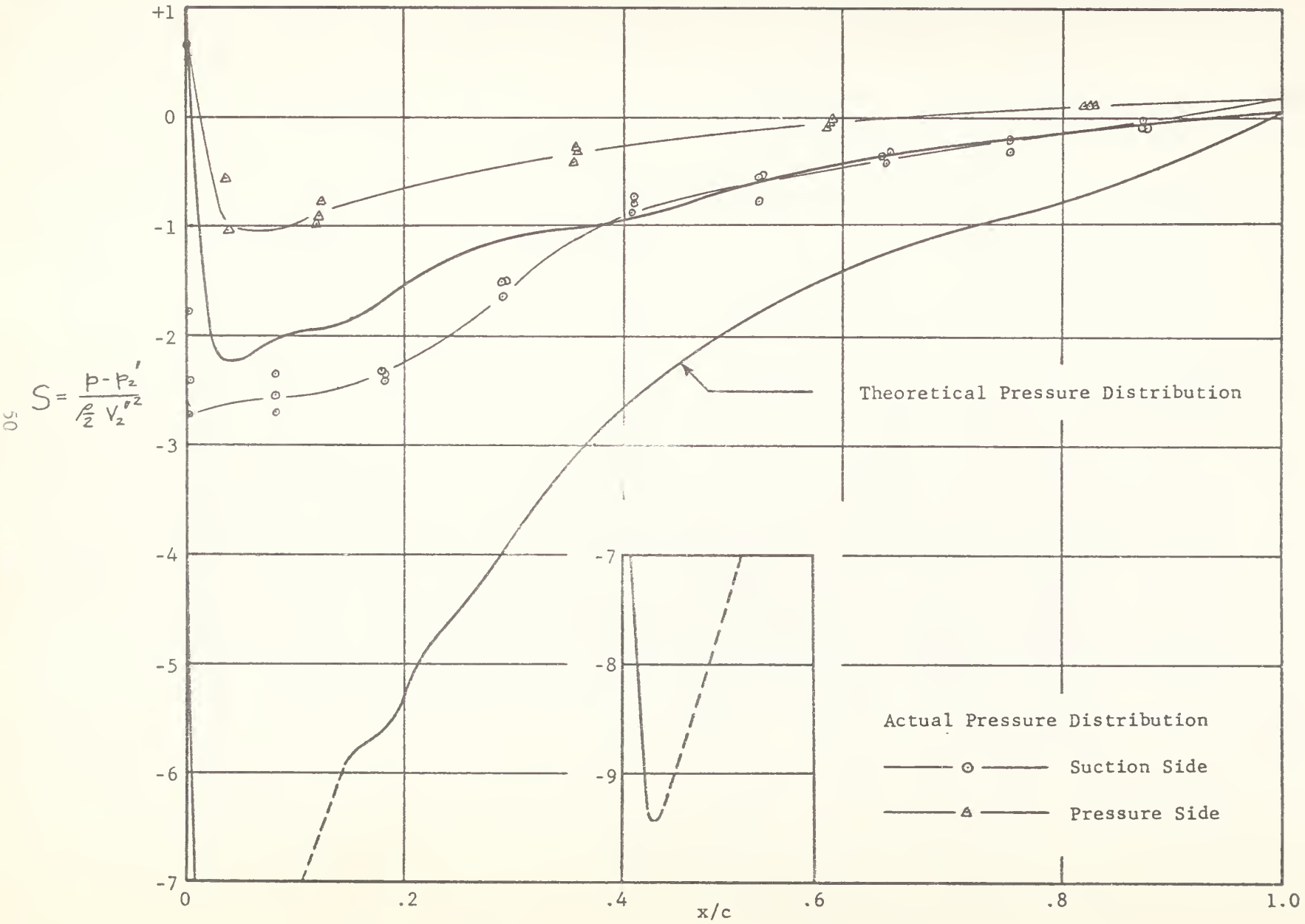

Fig. 6 Pressure Distribution around Blade Profiles for Ideal and Actual Flows with an Inlet Flow Angle of 58 degrees

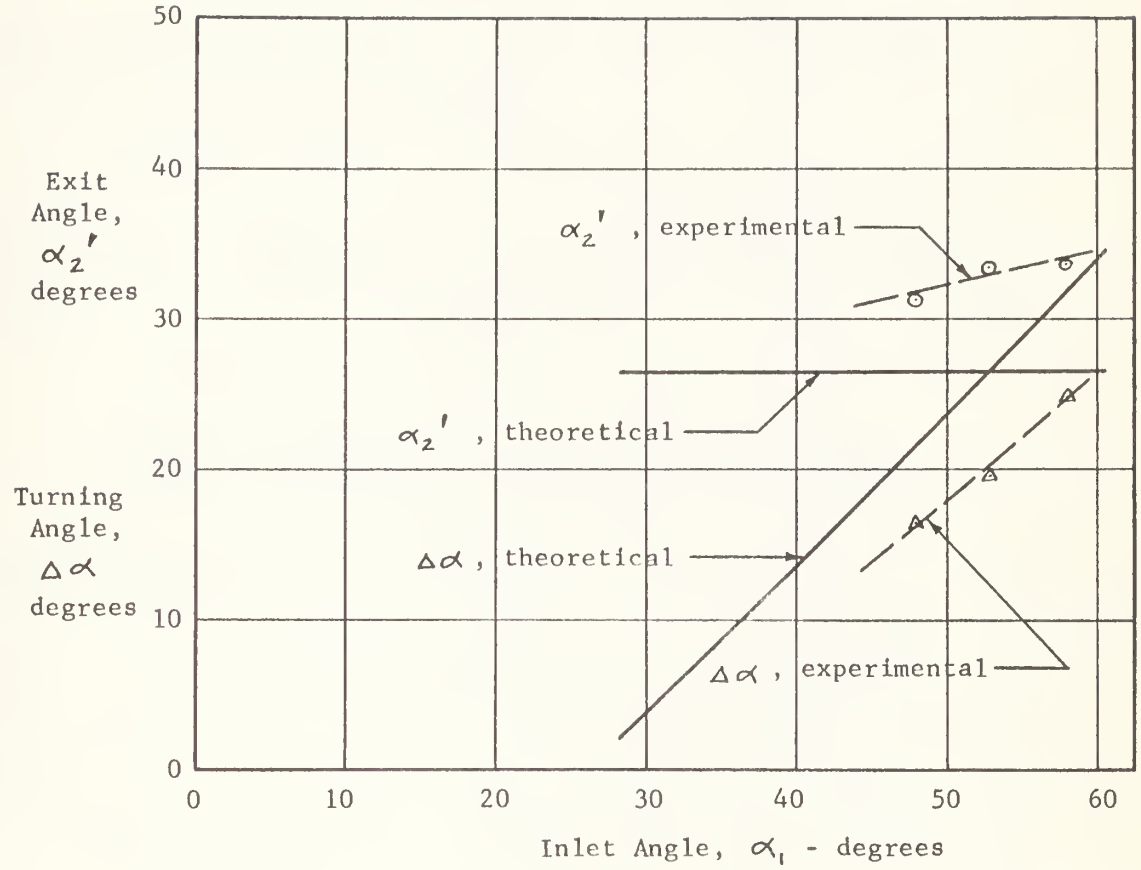

Fig. 7

Exit Angle and Turning Angle versus Inlet Angle
for Ideal and Actual Flow

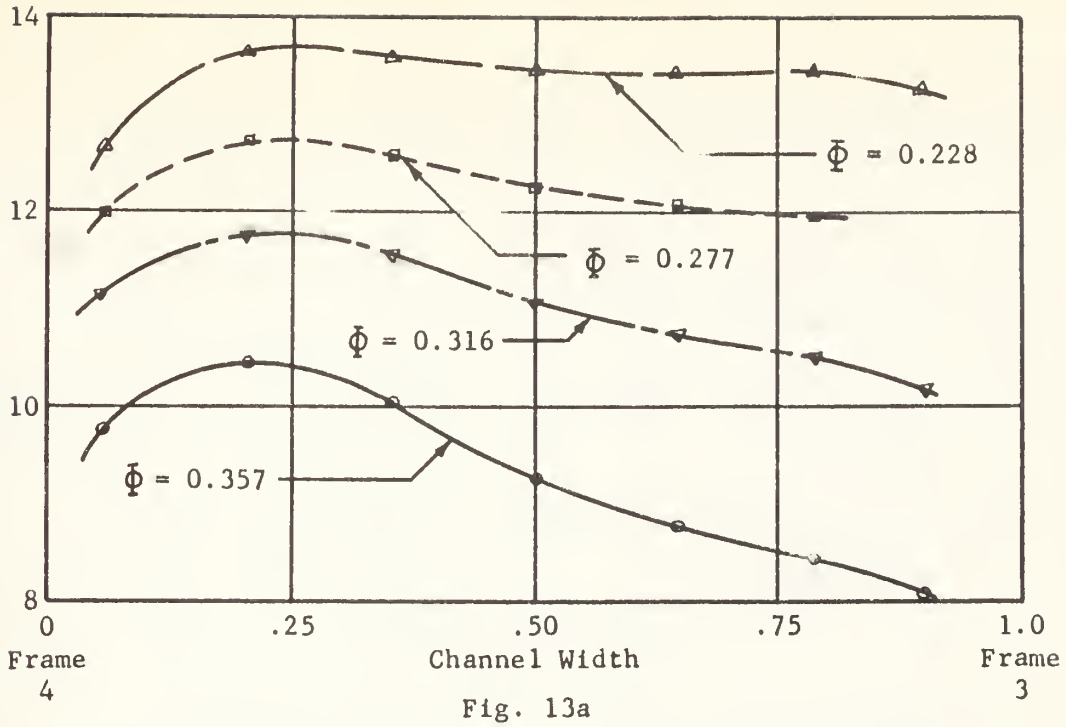

Fig. 13a

Fig. 13 Variation of Total Pressure and Flow Angle across Diffuser Channel at Cascade Inlet for four Flow Rates

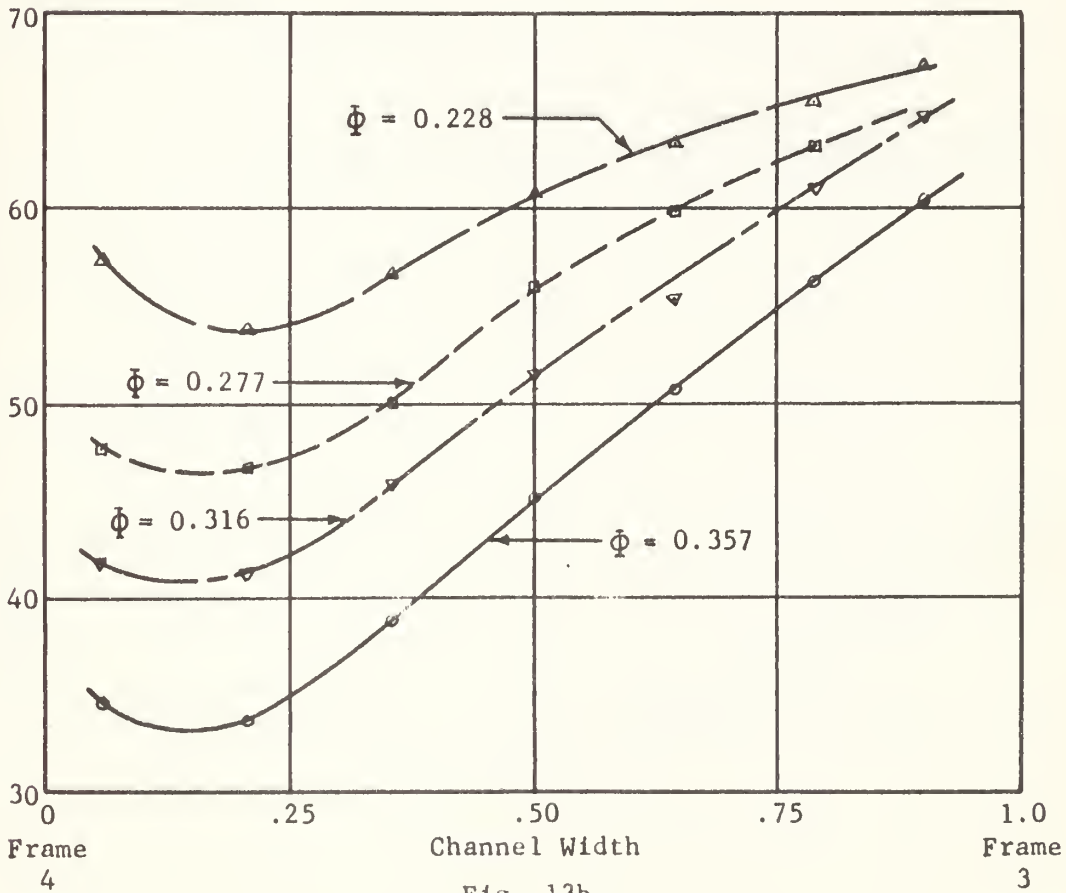

Fig. 13b

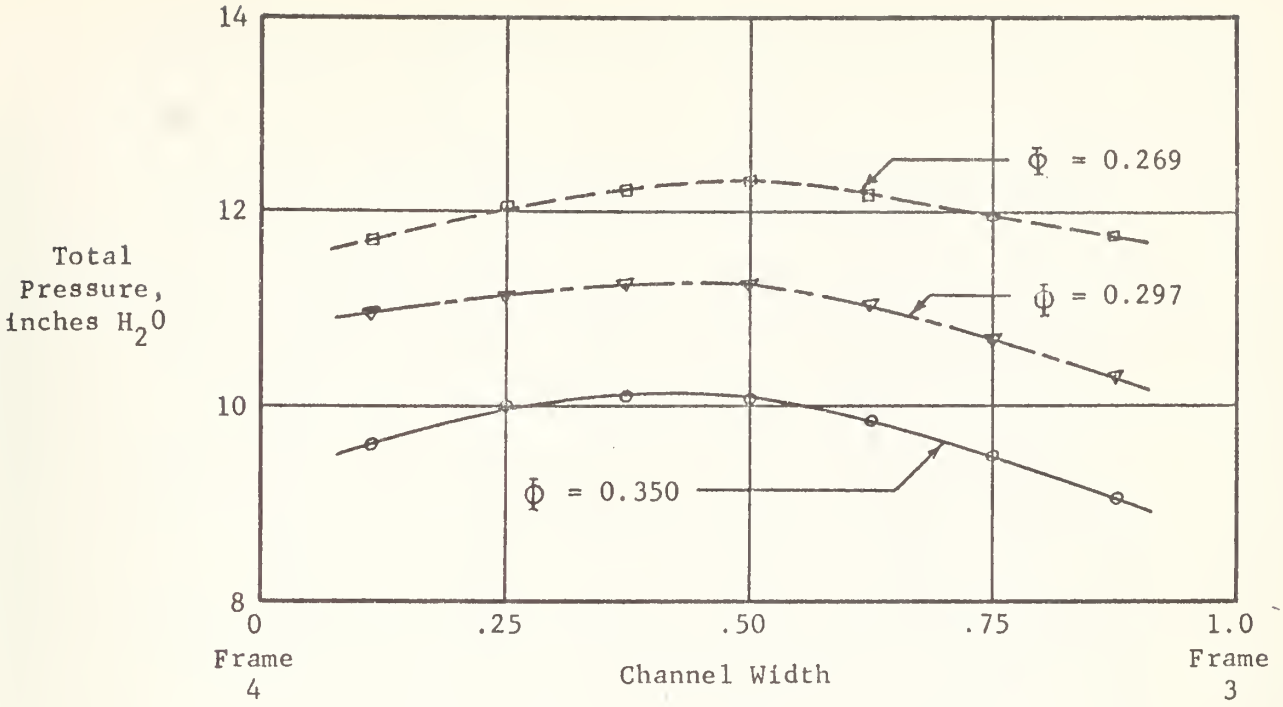

Fig. 14a

Fig. 14

Variation of Total Pressure and Flow Angle across Diffuser Channel at Fixed Circumferential Location in Cascade Wake for three Flow Rates

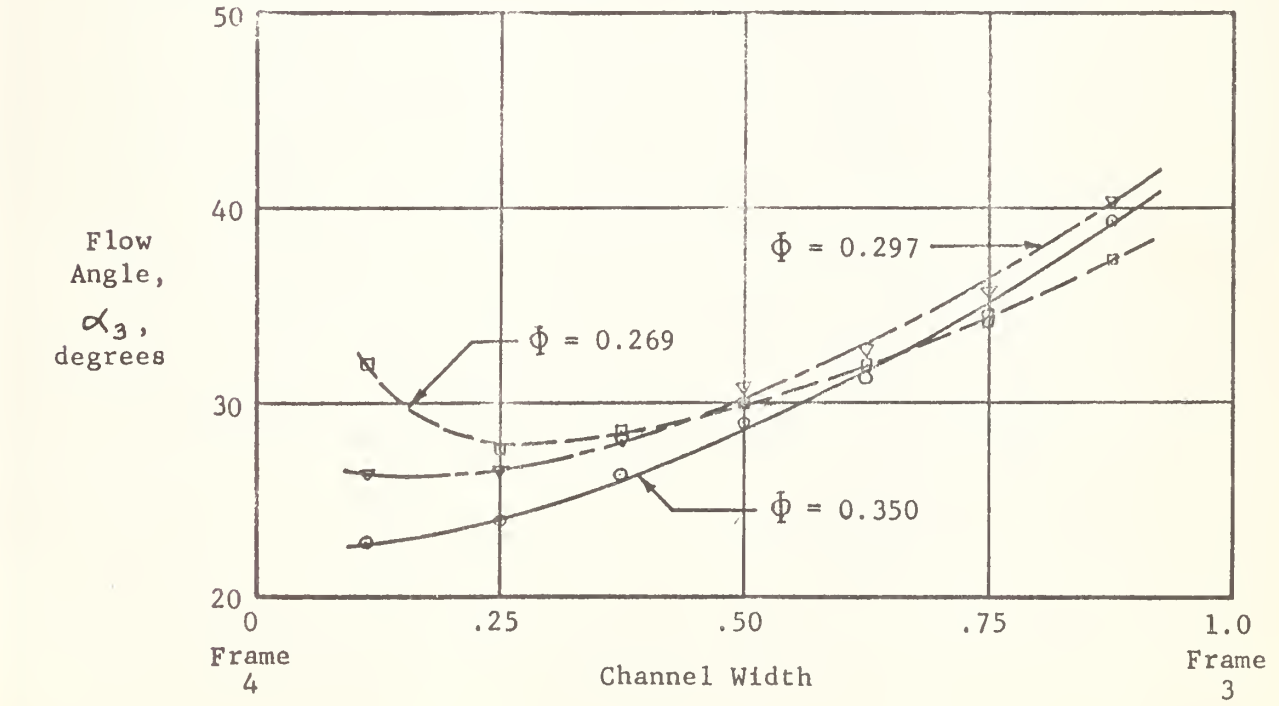

Fig. 14b

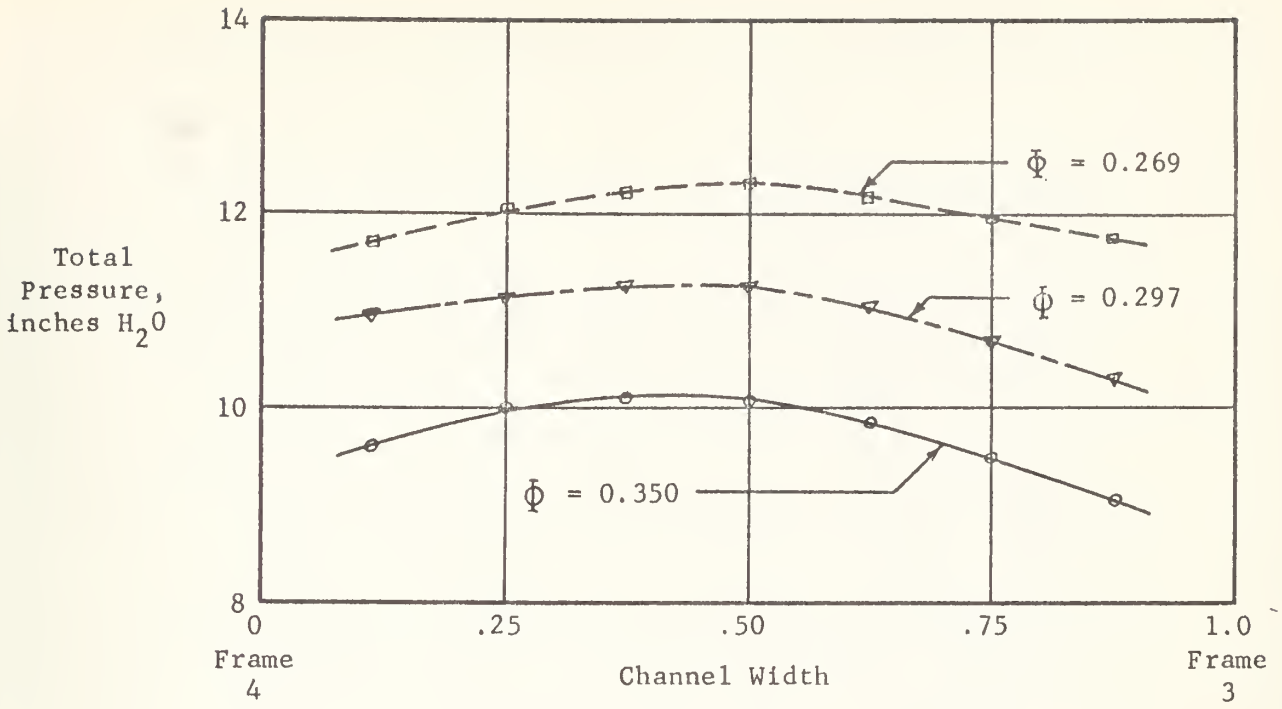

Fig. 14a

Fig. 14

Variation of Total Pressure and Flow Angle across Diffuser Channel at Fixed Circumferential Location in Cascade Wake for three Flow Rates

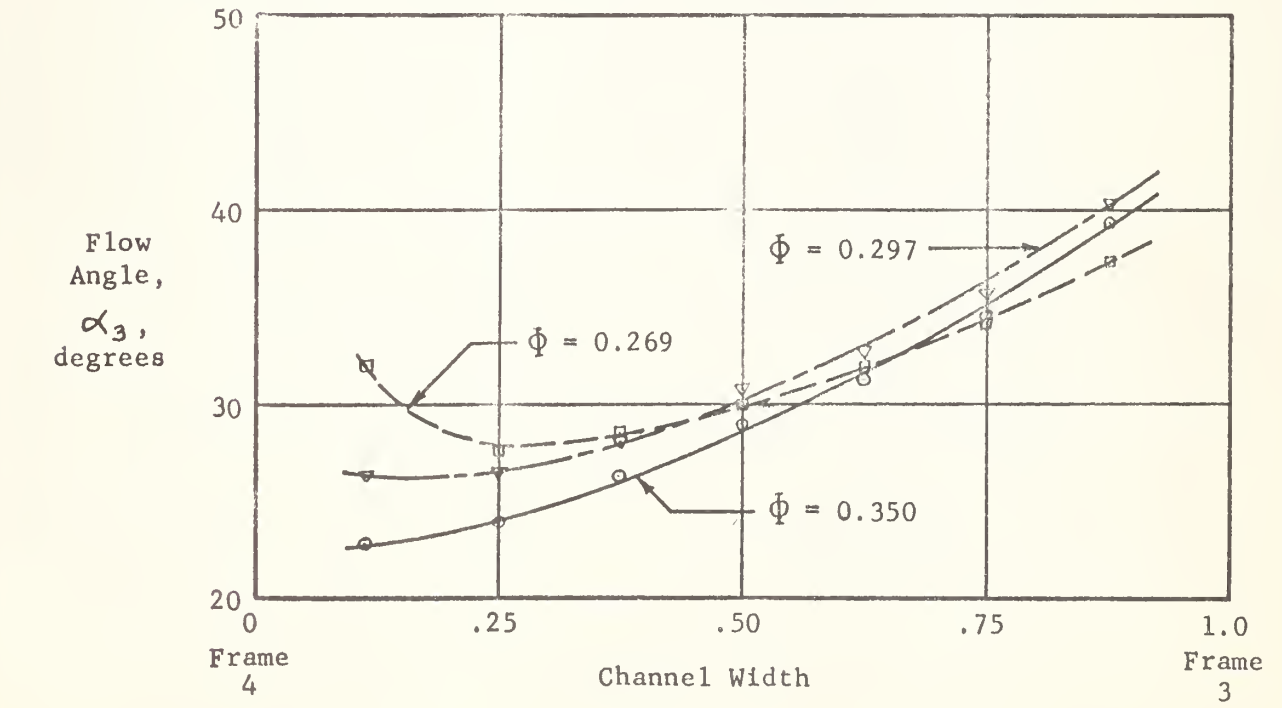

Fig. 14b

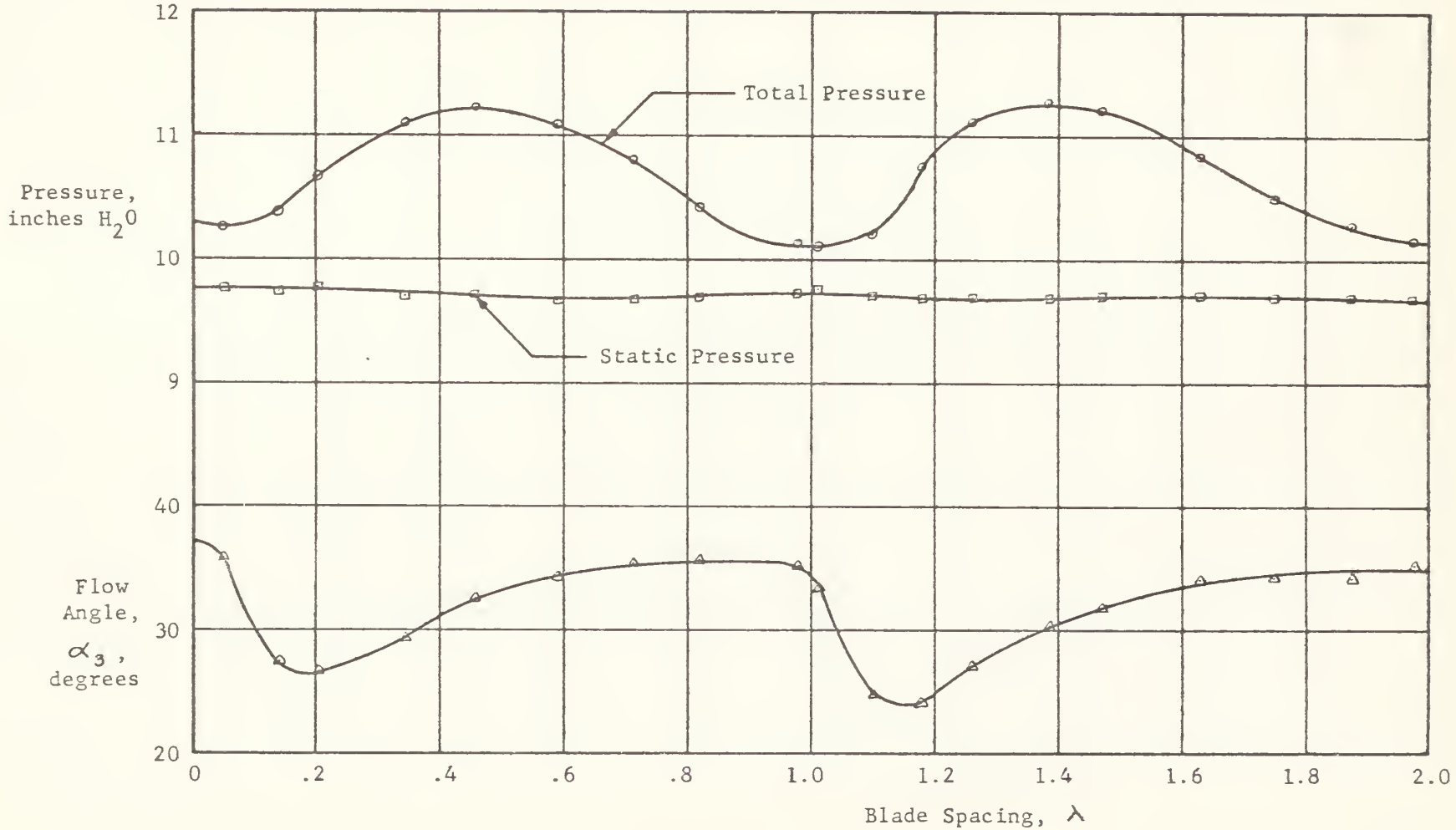

Fig. 15

Variation of Total Pressure, Static Pressure, and Flow Angle versus Blade Spacing in Cascade Wake with an Inlet Flow Angle of 53 degrees

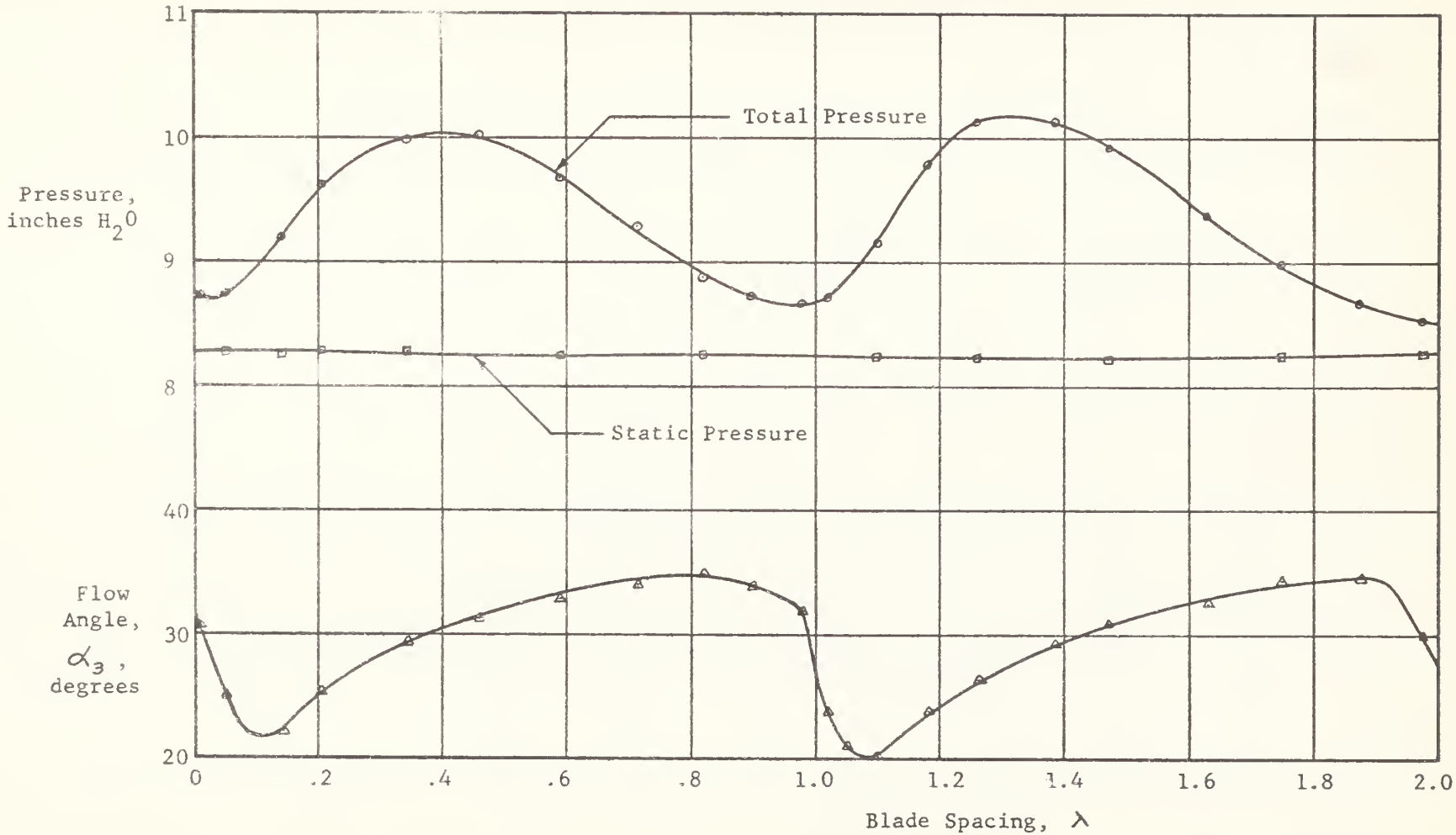

Fig. 16

Variation of Total Pressure, Static Pressure, and Flow Angle versus Blade Spacing in Cascade Wake with an Inlet Flow Angle of 48 degrees

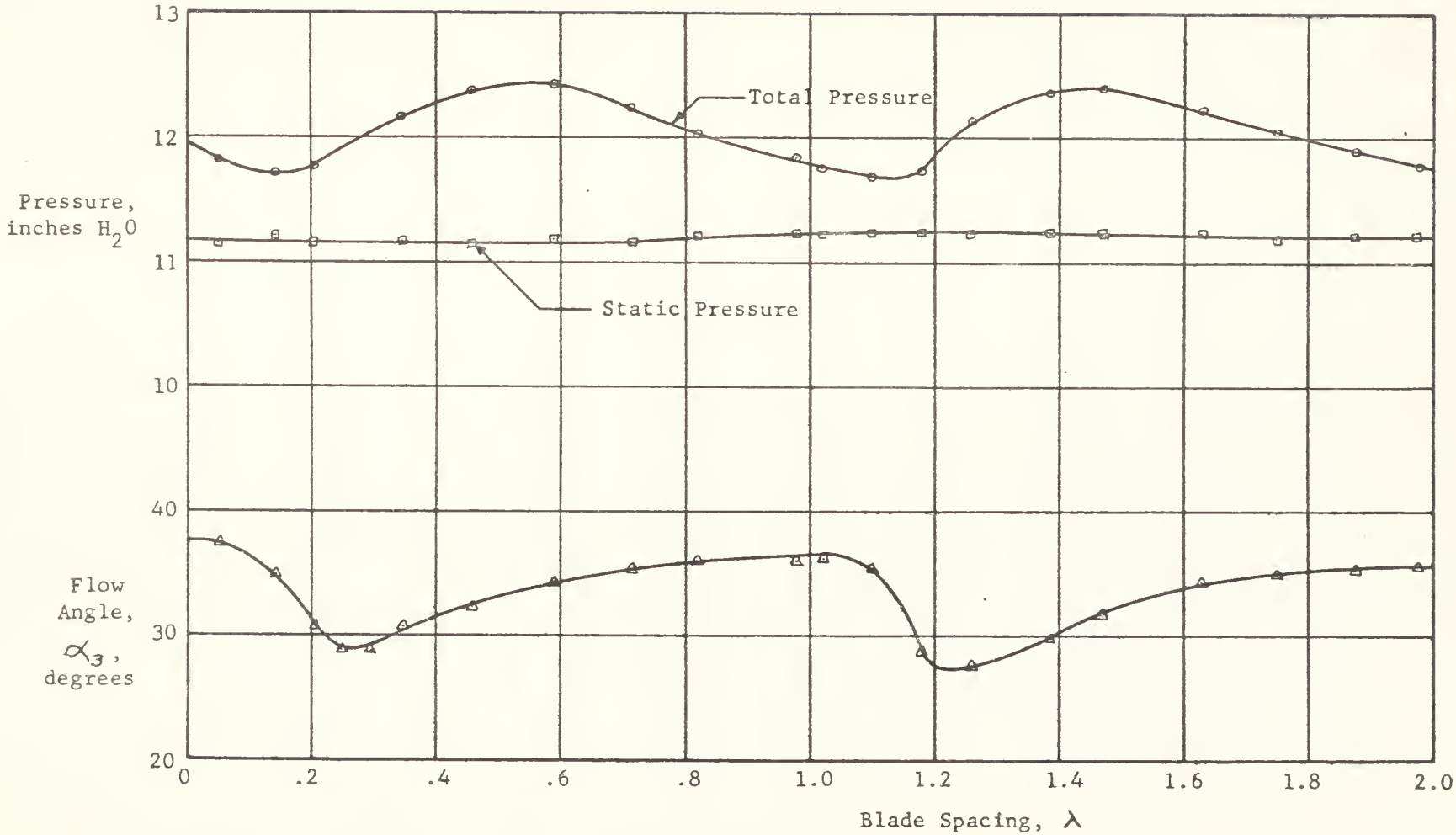

Fig. 17

Variation of Total Pressure, Static Pressure, and Flow Angle versus Blade Spacing in Cascade Wake with an Inlet Flow Angle of 58 degrees

APPENDIX A

TRANSFORMATION RELATIONS BETWEEN A RECTILINEAR CASCADE AND A CIRCLE

This appendix describes the calculating procedure for the determination of the pressure distribution around the blade profiles of a rectilinear cascade for potential flows using the data obtained from the electric analog field plotter. The relationship between inlet flow angle, exit flow angle, and cascade turning angle may also be calculated using the procedures described below. The information which must be known from the field plotter is,

ϕ_1 , ϕ_2 : The electrical potential at the two stagnation points M_1 and M_2 .

ϕ_T : The electric potential at the trailing edge of the blade profile.

$\left.\frac{\Delta\phi}{\Delta x}\right]_\infty = V_a$: The potential gradient near the bus bars, which is equivalent to the velocity perpendicular to the cascade axis infinitely far ahead or behind the cascade.

s : The spacing distance between each blade of the cascade.

ϕ and $\frac{d\phi}{dz}$: The electric potential and potential gradient at chosen points on the blade profile.

The dimensions of the ϕ , $\Delta\phi$, and $d\phi$ quantities may be either volts or percent of the total voltage between the bus bars. The dimensions of the Δx , s , and dz quantities may be expressed with arbitrary but equal scales. The quantity dz as used here is the differential increment of length along the surface of the blade profile. It is assumed that a specific value of α_∞ has been chosen. The

sign convention for the various quantities is as follows,

ϕ_1, ϕ_2, V_a, s, $\frac{dq}{dz}$: Positive in all cases.

ϕ_T, q : Positive for all locations on the surface of the blade extending from M_1 through P to M_2 as shown in Fig. 1.
Negative for all locations on the surface of the blade extending from M_1 through Q to M_2 as shown in Fig. 1.

α_∞ : Positive for angles extending below the line which is perpendicular to the cascade axis.

The intermediate quantity C is first calculated using the relation,

$$C = e^{\left[\frac{\pi(\phi_1 - \phi_2)}{2 s V_a}\right]} \qquad \text{A1}$$

then determine the quantity b, which locates the sources and sinks in the φ plane, from the relation,

$$b = \frac{C+1}{C-1} \qquad \text{A2}$$

Determine the fractional potential drop for the trailing edge point from,

$$f_{1_T} = \frac{\phi_1 - |\phi_T|}{\phi_1 - \phi_2} \qquad \text{A3}$$

and determine the corresponding location of the trailing edge point on the unit circle in the φ plane by,

$$\theta_T = \cos^{-1}\left\{A\left[\frac{1-B}{1+B}\right]\right\} \qquad \text{A4}$$

where $$A = \cosh \tau = \frac{1}{2}\left(b + \frac{1}{b}\right) \qquad \text{A5}$$

and $$B = \left[\frac{b-1}{b+1}\right]^{(4 f_{1_T} - 2)} \qquad \text{A6}$$

By definition, $\beta = \theta_T$, and the sign of β is determined by the sign of ϕ_T. Find $\sinh \tau$ from,

$$\sinh \tau = \frac{1}{2}\left(b - \frac{1}{b}\right) \qquad \text{A7}$$

and determine the quantity K from,

$$K = \frac{\sin \beta}{\sinh \tau} - \frac{\cos \beta \tan \alpha_\infty}{\cosh \tau} \qquad \text{A8}$$

The inlet and exit flow angles may be found from,

$$\alpha_1 = \tan^{-1}\left[\tan \alpha_\infty - K\right] \qquad \text{A9}$$

$$\alpha_3 = \tan^{-1}\left[\tan \alpha_\infty + K\right] \qquad \text{A10}$$

If it is desired to specify the inlet flow angle rather than α_∞ it will be necessary to calculate the values of α_1 for various values of α_∞ using equations A8 and A9. These values may be plotted and the correct value of α_∞ chosen to give the desired α_1.

To determine the values of θ and K for the selected points on the profile, use equations A3, A4, A5, A6, and A8 substituting ϕ, f_1, and θ for ϕ_T, f_{1_T}, and β. Then find,

$$f_2 = \frac{\sinh \tau \cos \theta}{\cosh \tau \sin \theta} \qquad \text{A11}$$

and $$f_3 = \frac{\sinh \tau}{\sin \theta} \qquad \text{A12}$$

The velocity at each point relative to the reference velocity V_2' may then be found from,

$$\frac{V}{V_2'} = \frac{d\phi/dz}{V_a} \cos\alpha_3 \left[1 - f_2 \tan\alpha_{m_2} \tan\alpha_2\right] \quad \text{A13}$$

and the pressure coefficient may be evaluated by,

$$S = 1 - \left(\frac{V}{V_2'}\right)^2 \quad \text{A14}$$

APPENDIX B

TRANSFORMATION OF A RECTILINEAR CASCADE TO A CYLINDRICAL CASCADE

This appendix describes a method of transforming a rectilinear cascade into a cylindrical cascade, including transformation of coordinates, and transformation of flow angles and blade profile pressure distribution for a given flow. The information which must be known for the rectilinear cascade includes the blade profile, blade spacing, blade stagger angle, flow angles, and the blade profile pressure distribution. The information which will be determined for the corresponding cylindrical cascade with a specified number of blades is the blade profile, blade stagger angle, flow angles, and the blade profile pressure distribution.

TRANSFORMATION OF COORDINATES

Let the rectilinear cascade exist in the z plane where

$$z = x + iy \tag{B1}$$

and let the cylindrical cascade exist in the w plane where

$$w = re^{i\theta} \tag{B2}$$

as shown in Fig. B1.

The transformation relation is

$$w = e^{\frac{2\pi}{sN} z} \tag{B3}$$

from which

$$r = e^{\frac{2\pi}{sN} x} \tag{B4}$$

and

$$\theta = \frac{y}{s} \frac{2\pi}{N} \tag{B5}$$

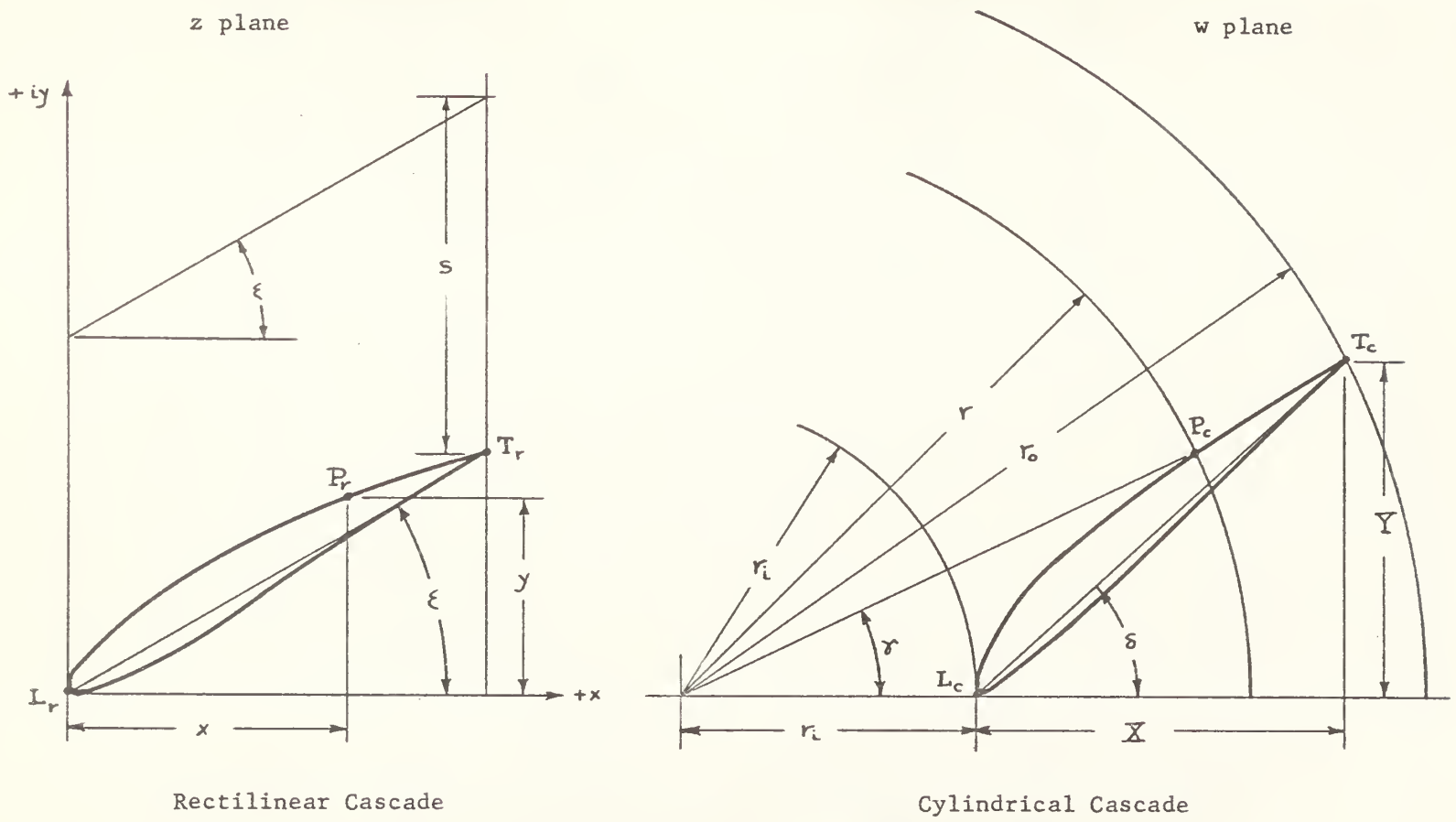

Fig. B1

Geometrical Parameters of the Rectilinear and Cylindrical Cascade

for $x = 0$, $r_i = 1$ B6

and for $x = x_T$, $r_c = e^{\frac{x_T}{s}\frac{2\pi}{N}}$ B7

The values for x and y are found using the following relationships as determined from Fig. B2,

$$x = \xi_r \cos\xi - \eta_r \sin\xi \quad \text{B8}$$

$$y = \xi_r \sin\xi + \eta_r \cos\xi \quad \text{B9}$$

where ξ_r and η_r are the profile coordinates as given with respect to the chord reference line. The blade spacing (s), ξ_r and η_r may be measured in any consistent units, although these distances are usually expressed in terms of chord length.

Having determined r and γ in the w plane for a given point, rectangular coordinates of that point can be found by

$$X = r\cos(\gamma) - r_i \quad \text{B10}$$

$$Y = r\sin(\gamma) \quad \text{B11}$$

The straight line between the transformed leading edge point (L_c) and the transformed trailing edge point (T_c) forms the new chord reference line, since the chord reference line of the rectilinear cascade transforms into a logarithmic spiral and a straight chord reference line is desirable. The angle (ζ) between the new chord reference line and a radial line is determined by

$$\zeta = \tan^{-1}\left[\frac{Y_T}{X_T + r_i}\right] \quad \text{B12}$$

Rectilinear Cascade

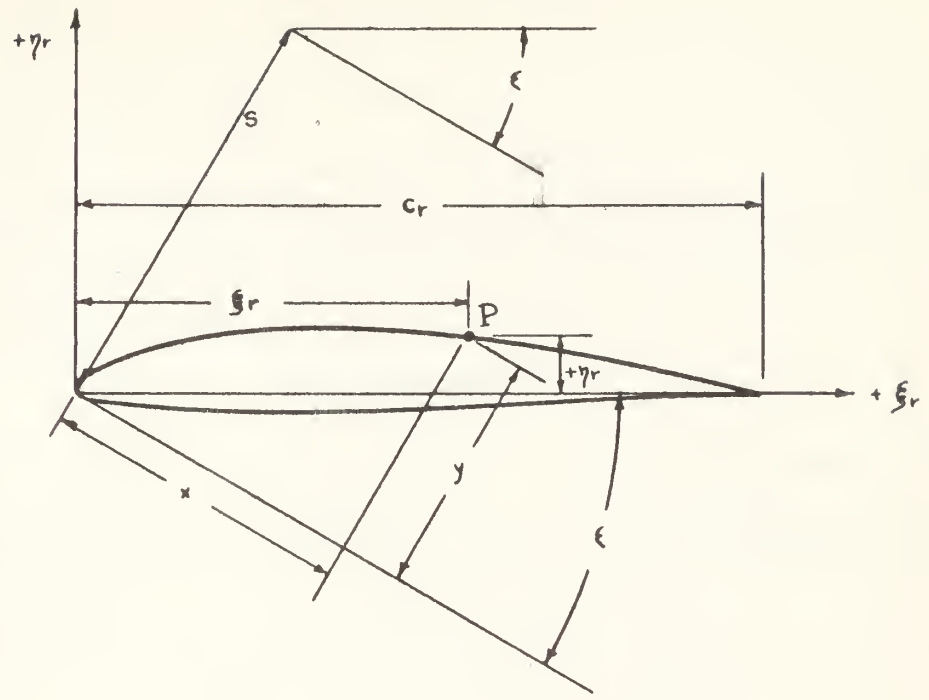

Cylindrical Cascade

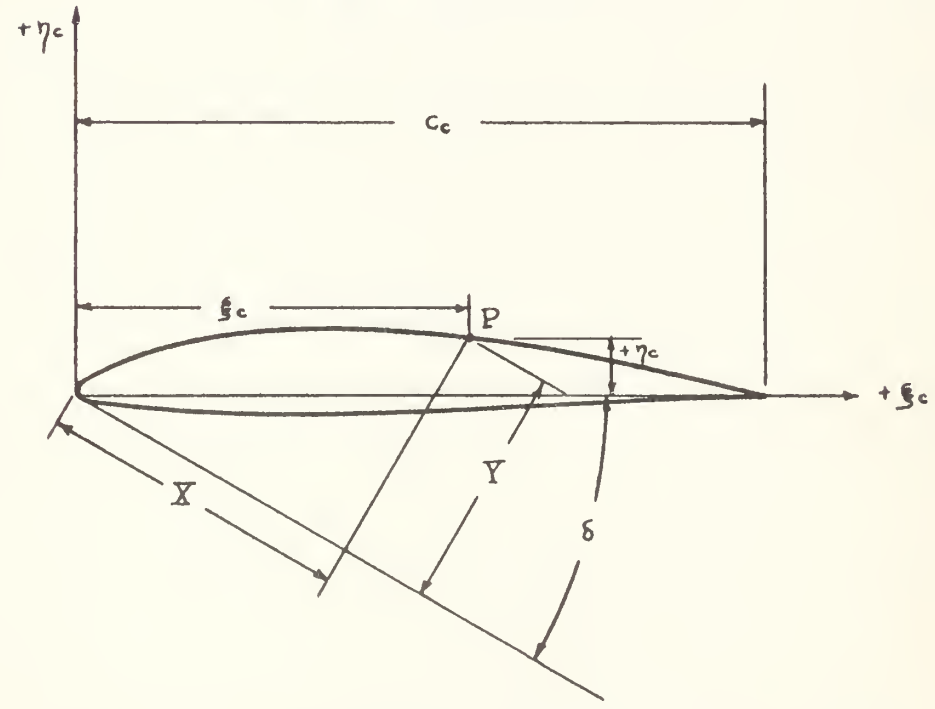

Fig. B2 Relationship between Profile Coordinate Axes and Cascade Parameters for the Rectilinear and Cylindrical Cascade

If airfoil coordinates with respect to the new chord reference line are desired,

$$\xi_c = X \cos\delta + Y \sin\delta \qquad \text{B13}$$

$$\eta_c = Y \cos\delta - X \sin\delta \qquad \text{B14}$$

and a suitable factor may be applied so that ξ of the trailing edge point equals 100%.

FLOW ANGLES

By the nature of this transformation, the flow angles ahead of and after the cylindrical cascade are equal to the flow angles ahead of and after the rectilinear cascade, respectively.

BLADE PRESSURE COEFFICIENTS

The blade pressure coefficient is defined as

$$S = \frac{p - p_2'}{\frac{\rho}{2} V_2'^2} \qquad \text{B15}$$

from which

$$S = 1 - \left(\frac{V}{V_2'}\right)^2 \qquad \text{B16}$$

The mapping derivative for this transformation is

$$\frac{dw}{dz} = \frac{2\pi}{sN} W \qquad \text{B17}$$

from which

$$\frac{V_2}{V_\infty} = \frac{2\pi}{sN} r \qquad \text{B18}$$

and

$$\left(\frac{V}{V_2'}\right)_c = \left(\frac{V}{V_2'}\right)_r \left(\frac{r}{r_2}\right) \qquad \text{B19}$$

From equations B16 and B19, the relationship between the blade pressure coefficients in the two planes is,

$$S_c = 1 - (1 - S_r)\left(\frac{r_2}{r}\right)^2 \qquad \text{B20}$$

If a rectilinear cascade is desired to be transformed into a cylindrical cascade with the leading edge of the blades at the outer radius, as in the case of inlet guide vanes, substitute for ξ_r the value $(C_r - \xi_r)$ in equations B8 and B9.

APPENDIX C

TRANSFORMATION OF A CYLINDRICAL CASCADE TO A RECTILINEAR CASCADE

This appendix describes a method of transforming a cylindrical cascade into a rectilinear cascade, including transformation of coordinates, and transformation of flow angles and blade profile pressure distribution for a given flow. The information which must be known for the cylindrical cascade includes the blade profile, number of blades, blade stagger angle, inner radius of cascade, flow angles, and the blade profile pressure distribution. The information which will be determined for the corresponding rectilinear cascade is the blade profile, blade spacing, blade stagger angle, flow angles, and the blade profile pressure distribution.

TRANSFORMATION OF COORDINATES

Let the cylindrical cascade exist in the w plane where

$$w = r e^{i\theta} \tag{C1}$$

and let the rectilinear cascade exist in the z plane where

$$z = x + iy \tag{C2}$$

as shown in Fig. B1.

The transformation relation is

$$z = \frac{sN}{2\pi} \log w \tag{C3}$$

from which

$$\frac{x}{s} = \frac{N}{2\pi} \log_e \left(\frac{r}{r_i}\right) \tag{C4}$$

and

$$\frac{y}{s} = \frac{N}{2\pi} \theta \tag{C5}$$

The parameters $\frac{r}{r_c}$ and γ are determined from the coordinates of the profile in the rectilinear plane, X and Y,

$$\frac{r}{r_c} = \sqrt{\left(1 + \frac{X}{r_c}\right)^2 + \left(\frac{Y}{r_c}\right)^2} \qquad C6$$

$$\gamma = \tan^{-1}\left[\frac{Y/r_c}{1 + X/r_c}\right] \qquad C7$$

where X and Y are determined from the conventional profile coordinates ξ_c and η_c as shown in Fig. B2,

$$X = \xi_c \cos\delta - \eta_c \sin\delta \qquad C8$$

$$Y = \xi_c \sin\delta + \eta_c \cos\delta \qquad C9$$

The stagger angle of the rectilinear cascade (ξ) is determined by

$$\xi = \tan^{-1}\left[\frac{y_T/r_T}{x_T/s}\right] \qquad C10$$

and the solidity (σ) is determined by

$$\sigma = \frac{c}{s} = \sqrt{\left(\frac{x_T}{s}\right)^2 + \left(\frac{y_T}{s}\right)^2} \qquad C11$$

Conventional coordinates of the rectilinear cascade profile may then be determined by,

$$\frac{\xi_0}{s} = \frac{x}{s}\cos\xi + \frac{y}{s}\sin\xi \qquad C12$$

$$\frac{\eta_0}{s} = \frac{y}{s}\cos\xi - \frac{x}{s}\sin\xi \qquad C13$$

and a suitable scale factor may be applied so that ξ of the trailing edge point equals 100%.

FLOW ANGLES

By the nature of this transformation, the flow angles ahead of and after the rectilinear cascade are equal to the flow angles ahead of and after the cylindrical cascade, respectively.

BLADE PRESSURE COEFFICIENTS

From equation B20 in the derivation of Appendix B,

$$S_r = 1 + (S_c - 1)\left(\frac{r}{r_2}\right)^2 \qquad \text{C14}$$

APPENDIX D

DETERMINATION OF THE REFERENCE STATIC AND DYNAMIC PRESSURE FOR THE ACTUAL FLOW

The following experimental data are known for the actual flow: Radius at which experimental data obtained, radius at which the reference static and dynamic pressure are desired, total pressure of flow, static pressure of flow, and flow density (determined from inlet conditions and assumed to remain constant.) These data are measured in the plane of the center pressure taps. From this information the velocity, radial velocity component, and tangential velocity component can be determined for each data point.

It is now desired to describe a uniform flow that has the same mass flow rate and the same tangential momentum flow as the measured flow and which is located at the same radius. From the Law of Conservation of Mass, the radial velocity component is determined by,

$$V_{R_3}' = \int_0^{\lambda} V_{R_3} \, d\lambda \qquad \text{D1}$$

where λ is that portion of the circumferential arc, in the plane of the center pressure taps, corresponding to one blade space. From the Law of Conservation of Momentum, the change in static pressure is determined by,

$$p_3' - p_3 = \rho \left[\int_0^{\lambda} (V_{R_3})^2 \, d\lambda - (V_{R_3}')^2 \right] \qquad \text{D2}$$

where pressure is expressed in pounds per square foot, density in slugs per cubic foot, and velocity in feet per second. From the Law of Conser-

vation of Momentum, the tangential velocity component is determined by,

$$V_{t_3}' = \frac{1}{V_{R_3}'} \int_0^1 (V_{R_3} \, V_{z_3}) \, dA \qquad \text{D3}$$

The flow angle is determined by,

$$\alpha_3' = \tan^{-1}\left[\frac{V_{t_3}'}{V_{R_3}'}\right] \qquad \text{D4}$$

The uniform flow is now described by its density, velocity, static pressure, and flow angle. From these conditions the uniform flow total pressure can be determined.

Assuming a constant total pressure, the velocity of this uniform flow as it would exist at the radius of the trailing edge of the cascade blades, is determined by,

$$V_2' = V_3'\left(\frac{r_3}{r_2}\right) \qquad \text{D5}$$

The flow angle of the uniform flow does not change with the change in radius,

$$\alpha_2' = \alpha_3' \qquad \text{D6}$$

Knowing the velocity, density, and total pressure of the uniform flow, the static pressure and dynamic pressure can easily be determined.

For this investigation, the integrals of Equations D1, D2, and D3 were evaluated by graphical means. The integrations were performed using data obtained from measurements along the arc corres-

ponding to two blade spaces in an attempt to more accurately determine the cascade exit conditions.